

Abstract

English:

This master's thesis project deals with the control and the regulation of the temperature inside the fermentor of a biogas demonstration system. The project consists of a complete engineering approach through identification of problems, the modeling of the system, the designing of the control solution, its implementation and the discussion of results.

The model, representing the thermal transfers, was implemented in Simulink for analysis purposes and the solution was implemented using the LabView software. The advantages and drawbacks of the new solution are discussed and several avenues of improvement are suggested to.

Français:

Ce travail de fin d'étude traite du contrôle et de la régulation de la température à l'intérieur du fermenteur d'un système de démonstration de production de biogaz. Le projet présente une démarche d'ingénieur globale à travers l'identification du problème, la modélisation du système, le design de la solution de contrôle, son implémentation et la discussion des résultats.

Le modèle, représentant les échanges thermiques, est implémenté dans Simulink à des fins d'analyses et la solution a été implémentée grâce au logiciel LabView. Les avantages et inconvénients de la nouvelle solution sont expliqués et des pistes d'améliorations sont suggérées à la fin de cet ouvrage.

Acknowledgments

First of all, I would like to thank Zhenyu Yang for all the knowledge he has shared with me, for helping and advising me throughout my thesis, and for giving me the technical support and the general lines of the project.

Furthermore, I would like to thank Heidi Valdkilde Jensen and Peter Kringhøj for helping me with administrative procedures, for accommodation and for being the contact persons during my entire stay.

I want to also thank Austin Ehimen for his support in the bio-chemical field, helping me to fix the objectives of my thesis, and Henry Enevoldsen for his concern when I had a technical problem and for all the information he gave me.

Many thanks to Nathalie Vetcour for accepting to be in charge of my Master Thesis, as Gramme mentor.

Special thanks to Sonia Minelli and Christian Charlier, the international team of Helmo Gramme, for helping and advising me in my Erasmus applications and administrative procedures.

Thank you to Aalborg University Esbjerg for its facilities, support, library and accommodation

Last but not least, I would like to thank my family for their moral support throughout my studies and particularly for supporting me in my wish to experience an international internship.

Preface

Aalborg University, Esbjerg campus, disposes of a biogas demonstration plant for experimental purposes. In this kind of facility, temperature is an essential parameter and should be kept constant at an appropriate value for chemicals efficiency reasons.

With the existing equipment, a control system for temperature already existed but its performance has been really limited and no documentation to get it working was available.

In this context, it was decided to revise the control system. Furthermore, it has been decided to change the control strategy and to re-conceive the control system as a whole. So, the new results should be compared with those of the previous system.

Table of Content

| | |
|---|------------|
| ABSTRACT | II |
| ACKNOWLEDGMENTS | III |
| PREFACE | IV |
| TABLE OF CONTENT..... | V |
| 1. INTRODUCTION | 1 |
| 2. GENERAL BACKGROUND | 2 |
| 2.1. GENERALITIES ABOUT BIOGAS | 2 |
| 2.2. PRESENTATION OF THE PROCESS | 5 |
| 3. PROBLEM IDENTIFICATION | 14 |
| 3.1. THE EXISTING PROGRAM | 14 |
| 3.2. OBJECTIVES OF THE THESIS | 14 |
| 4. FEASIBILITY ANALYSIS | 16 |
| 4.1. BOILER COMMUNICATION..... | 16 |
| 4.2. BOILER CALIBRATION | 17 |
| 5. MODELING THE SYSTEM | 19 |
| 5.1. INTRODUCTION | 19 |
| 5.2. FIRST FERMENTOR MODEL | 20 |
| 5.2.1. <i>Modeling the Fermentor</i> | 20 |
| 5.2.2. <i>Determining the parameters for the fermentor demonstration system</i> | 24 |
| 5.3. SECOND FERMENTOR MODEL..... | 28 |
| 5.3.1. <i>Modeling the Losses</i> | 28 |
| 5.3.2. <i>Identification of the fermentor transfer function</i> | 32 |
| 5.3.3. <i>Remembering the hypotheses</i> | 38 |
| 5.3.4. <i>Determining the parameters of the transfer function</i> | 39 |
| 5.4. THE BOILER MODEL | 44 |
| 5.4.1. <i>Modeling the Boiler</i> | 44 |
| 5.4.2. <i>Determining the heater transfer function</i> | 48 |
| 5.4.3. <i>Determining the parameters for the boiler</i> | 50 |
| 5.5. THE PIPES MODEL | 54 |
| 5.5.1. <i>Modeling the pipes</i> | 54 |
| 5.5.2. <i>Identification of the transfer function of the pipe</i> | 56 |
| 5.5.3. <i>Determining the parameters of the pipe</i> | 56 |
| 5.6. MODELING THE TRANSFER FUNCTION OF T_2 | 57 |
| 5.7. CONCLUSION..... | 58 |
| 6. CONTROL DESIGN | 60 |
| 6.1. GLOBAL SCHEME SIMPLIFICATION | 60 |
| 6.2. PID GENERALITIES..... | 63 |
| 6.3. CLOSED LOOP..... | 66 |
| 6.4. PERFORMANCE REQUIREMENTS..... | 67 |
| 6.5. P ANALYSIS AND THE MODEL ERROR | 68 |

| | | |
|---------------------------|------------------------------------|-----------|
| 6.6. | PI ANALYSIS..... | 71 |
| 7. | IMPLEMENTATION | 74 |
| 7.1. | PREVIEW | 74 |
| 7.2. | FIRST RESULTS..... | 75 |
| 7.3. | TRYING TO IMPROVE THE DESIGN | 77 |
| 7.4. | TESTING THE IMPROVEMENTS | 79 |
| 7.5. | COOLING BEHAVIOR | 80 |
| 8. | CONCLUSIONS..... | 82 |
| 8.1. | RESULTS DISCUSSION | 82 |
| 8.2. | PERSONAL ASSESSMENT | 83 |
| ANNEX..... | | 85 |
| ANNEX 1 : | PROGRAMS FILES..... | 85 |
| ANNEX 2 : | EXAMPLE OF A NON-LINEAR MODEL..... | 85 |
| ANNEX 3 : | LIST OF TASKS COMPLETED..... | 89 |
| BIBLIOGRAPHY | | 91 |

1. Introduction

After a presentation of biogas generalities and about the facilities available, the existing control system will be dealt in more detail in order to explain the new strategy of control used for this thesis. Thus, the objectives of the thesis will be defined.

After that, a feasibility analysis will be the occasion to present the equipment at our disposal to implement the solution.

The next step will be the biggest, the complete system will be modeled in order to lead to a block diagram representing the whole plant. All the parameters of the model will be determined in this section and the model will be implemented in Simulink for the analysis purposes of analysis.

By means of this model, the design of a PI controller will be tackled and a solution will be implemented on the real system, using the LabView software. A critical evaluation of the results will be processed and an improvement of the solution will be experimented.

In the conclusion, the results of the solution are discussed and some avenues to improve the tuning of the PI controller are proposed.

NB : In this work, all the graphs representing temperatures are shown with the Y axis representing the temperature in °C and the X axis representing the time in seconds.

2. General Background

2.1. Generalities about Biogas

Although the thesis is oriented towards control systems and regulation, it seems useful or even essential to put the process in its context and to acquire some knowledge in the field of the process, i.e. biogas production.

The purpose of the process to be controlled is the production of biogas. Biogas is the renewable and biological version of natural gas. Indeed, biogas is produced by the fermentation of organic material: microorganisms are used to break down biodegradable material in the absence of oxygen and biogas is given off as a waste product of the reaction. This biochemical reaction is called fermentation and is a form of anaerobic digestion. The biogas generated during such a reaction is typically made up of methane (40 to 70% by volume) and carbon dioxide (30 to 60%). Variable quantities of water vapor and hydrogen sulfide can also be generated.

Biogas energy essentially comes from the fraction of methane. That's why biogas is usually purified to obtain biomethane. This methane is the same as that found in natural gas and that's why biomethane can be used in the distribution network of natural gas. Indeed, natural gas composition differs from biogas only in its by-products. So, biomethane can be used as a fuel for engines, gas turbines, boilers, industrial heaters, and in other processes, just as well as natural gas.

Since biogas is produced by the fermentation of organic material, several forms of products can be used to feed a biogas process:

- Crops: such as corn, but wild plants can also be used. Indeed, using food crops presents disadvantages presented later in this document. That's why the use of non-food crops have already been extensively cultivated and evaluated for the purpose of biogas production purpose. "Miscanthus", "switchgrass" and "short rotation coppice" are examples of such non-food plants.
- Rubbish dumps : their efficiency depends on their composition and on their tightness

- Collection of putrescible wastes
- Mud from water treatment plants
- Manure from breeding
- Certain industrial organic wastes
- Bottom of lakes and algae

Anaerobic digestion is a four-step process (Hydrolysis, Acidogenesis, Acetogenesis, Methanogenesis) schematically represented in Figure 1, for information. The curious reader will be able to find more information about this four-step process in the source indicated with the figure.

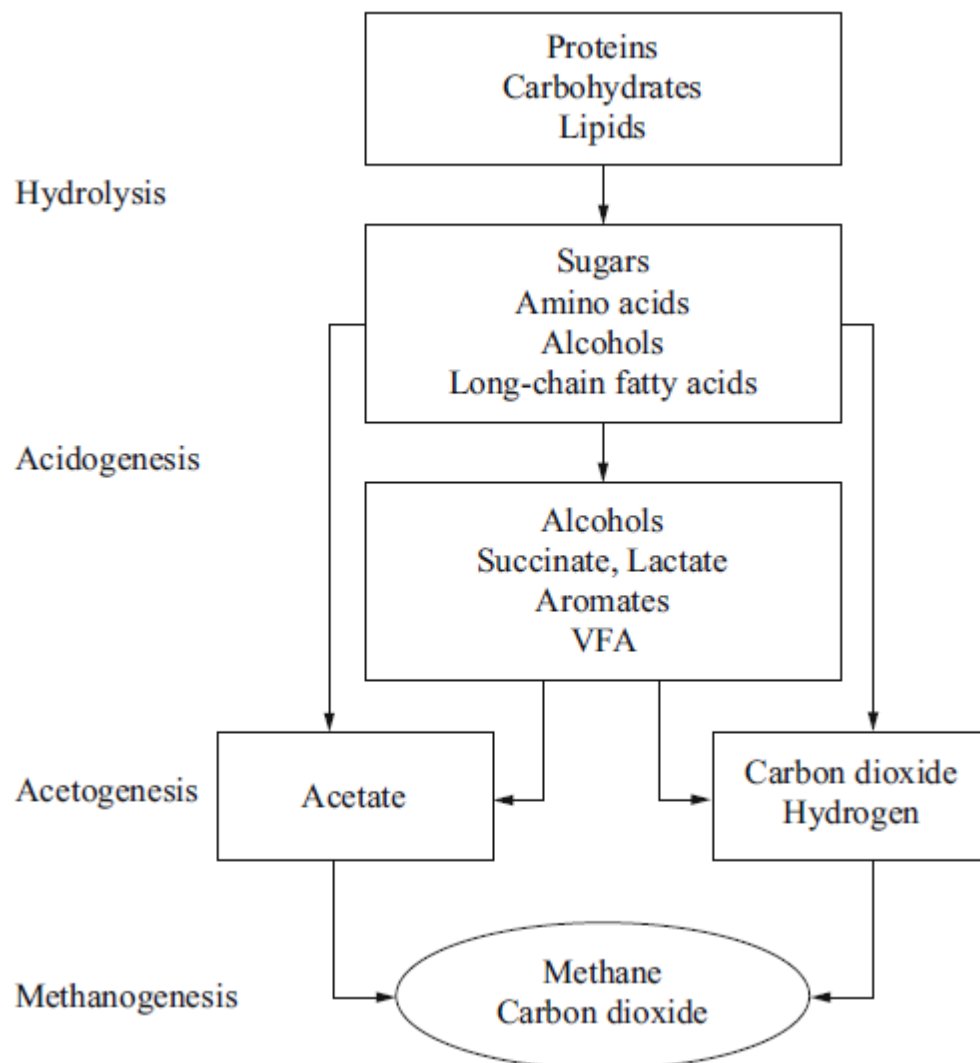


Figure 1 : Simplified conversion processes in anaerobic digestion¹

¹ (DEMIBRAS, 2009)

During the first days of an anaerobic digestion, the production of biogas is non-existent. After the first 6 days, the production increases exponentially. After 16 days, it reaches a plateau value and at the end of the 20th day, the digestion has reached the stationary phase.

Maximum daily biogas production takes place during 4 and 6 days and about 80 to 85% of the biogas production is generated between days 15 and 18.

Anaerobic digestion can occur within a wide range of environmental conditions. However, really specific conditions are needed to reach optimum production. The key parameters intervening in the stability and efficiency control are: temperature, pH, hydraulic retention time (HRT), organic loading rate (OLR), inhibitor concentration, concentrations of total volatile fatty acid (TVFA), and substrate composition.

The most important of these parameters is temperature. Anaerobic digestion can occur in a very large range of temperature, going from 10°C to 71°C. However, two specific regimes have been noted at optimal temperatures: the so-called mesophilic regime, at around 35°C and the thermophilic regime, at around 53°C. The thermophilic regime implies a higher biogas production rate but it needs a greater energy supply because anaerobic bacteria do not generate sufficient heat. It may also be important to note that biogas production falls off significantly between 39,4°C and 51°C and above 55°C.

Concerning the relationship between the amount of carbon and nitrogen present in the organic material (C/N ratio), microorganisms need a 20-30:1 ratio of C to N. However, agricultural residues contain low nitrogen levels and have a ratio around 60-90. That's why nitrogen needs to be supplemented, for example with ammonia (inorganic form) or with manure, urea or food wastes (organic form). But this issue can also favor the use of fertilizer for crops intended for biogas production.

Although biogas is composed of two greenhouse gases, its use is quite neutral from a greenhouse effect point of view because its production enters in the carbon cycle: the use of biogas only releases in the atmosphere the carbon which has already been taken out of the atmosphere by vegetal plants before. Anaerobic digestion can be

compared with respect to a number of environmental effects and sustainability criteria including energy balance, nutrient recycling, global warming mitigation potential, and so on. However, this consideration is theoretical and a study about the effect of biogas on the environment should take into account the human work needed to produce biogas and the total consumption of the production line. Multiple studies have been carried out but they lead to radically different results and conflicting conclusions.

However, a general conclusion can be set up concerning the raw materials used to produce biogas... Indeed, it seems that the biogas produced from agricultural residue, manure or food wastes has a much lower impact on the environment than biogas produced from crops dedicated to its production. Biogas from dedicated crops has a higher greenhouse global effect but also leads to other environmental and social problems like deforestation, increasing pressure on arable lands, increasing the demand and thus the price of food (which leads to famines), rebound effect on the use of fuel, and so on.

As a conclusion to this issue, it appears that it is really important to consider the provenance of biogas in order to judge its environmental effect: crops dedicated to biogas production and the use of food crops have a really bad impact on the environment while biogas from agricultural residue, manure or food wastes come within the scope of sustainable development and recycling. From this perspective, the first and the second generation of biogas (and generally, of biofuels) are differentiated. The first generation of biofuels depends on vegetal organs which are also used for human food, such as cereal seeds. The second generation uses the whole plant, so it is possible to use agricultural residues, such as stems, to produce biogas. Thus, the second generation can be used to upcycle food wastes and agricultural residues in a sustainable development context. That's why biofuels may be an important energy source in the future. The political bodies should promote the second generation of biofuels more and more around the world and the technological breakthroughs in this area should lead to a more and more sustainable process.

2.2. Presentation of the Process

This section will present facilities available for the realization of this thesis.

First of all, the reactor, also called the fermentor, consists of a glass vessel with a capacity of 5 liters. It is in this tank that the anaerobic digestion takes place under thermophilic conditions (53°C) but different fermentations, where the temperature do not exceed 60°C can also be carried out. The process can run with a wide range of feedstock, with varying solid content.

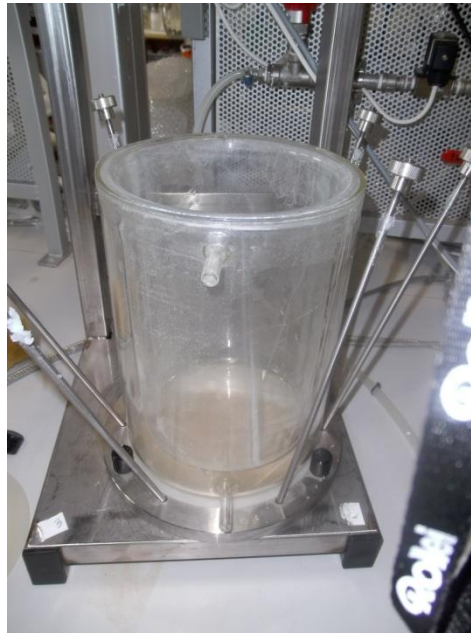


Figure 2 : The fermentor

The vessel presents a hollow partition where hot water can flow in order to heat the system.



Figure 3 : The hollow partition of the vessel

The regulation of the flow rate of the hot water in this hollow partition allows the user to control the temperature in the core of the reactor.

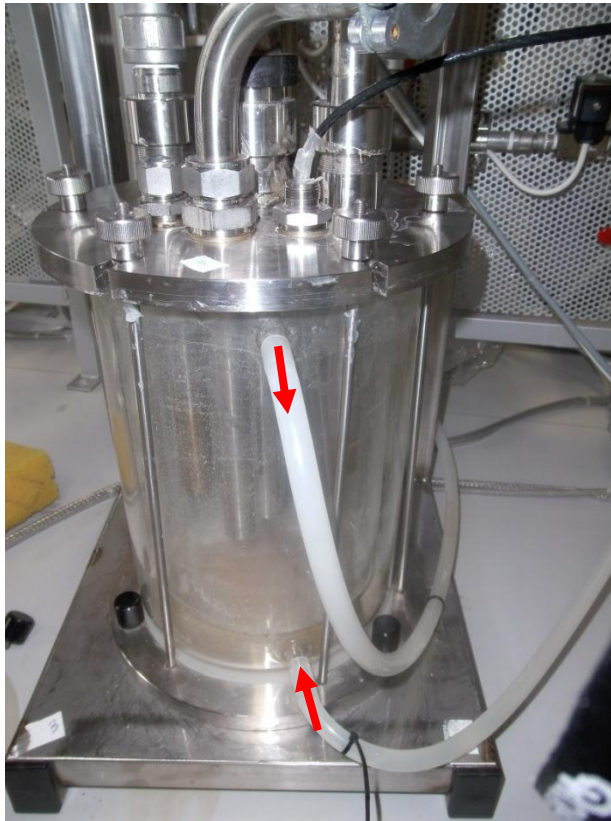


Figure 4 : Inputs and outputs for the heating water

This water heating supply is delivered by a circulation bath (called “boiler”) which ensures both the role of pump and of heater. Indeed, this device allows the user to choose the pressure and steady-state temperature for the water. The temperature control is assured by a PID controller and a heating resistance. In standard operating conditions, it is recommended to set the boiler temperature at 60°C, that is 7°C higher the fermentor temperature, to compensate for the energy losses in the water loop.



Figure 5: The circulation bath

The flow rate of the circuit is regulated by a proportional electro-valve controlled by Labview. This electro-valve needs a PMW input signal to control the opening of the valve (from 0 to 100%). That's why an electronics control is placed before the electro-valve in order to convert the analog output from LabView (from the computer) to an appropriate PMW signal for the electro-valve.



Figure 6: The Electro-valve



Figure 7: The PWM converter

A second valve is placed on the circuit to control manually the flow rate thanks to a PI controller. Indeed, this controller allows the user to control the valve opening manually (entering the opening in percent).

An automatic mode is also present to control this valve but it is not used for this project.



Figure 8 : The PI controller for the second valve

The feeding of the reactor is done by means of a pump which is able to pump liquid as well as solid particles, such as seeds. At present, the fermentor is fed discontinuously. This pump can also be used to empty the reactor.



Figure 9: The feeding pump

The fermentor is also implemented with a stirring system. This system can rotate from 0 to 11 rpm with a torque of 1Nm.

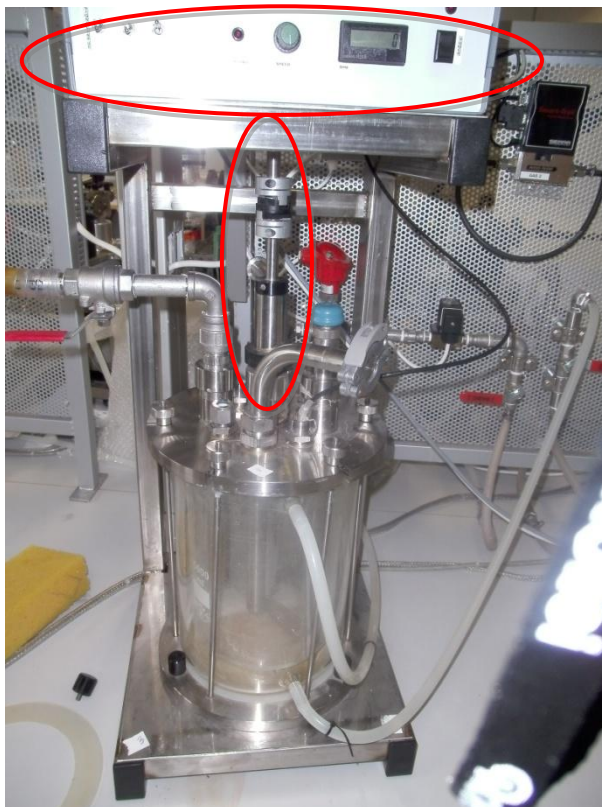


Figure 10 : The stirring system



Figure 11: The blade of the stirring system

A screwed lid is used on the top of the fermentor to ensure anaerobic conditions. The gas output is a continuous stream and is easily extracted through the output pipe.



Figure 12 : The output pipe

Pt100 temperature sensors are available to check the temperature of the ambient air or at the core of the fermentor. Another temperature sensor is situated in the water loop, a few decimeters after the fermentor water-output. Transmitters are used to convert resistance variations to voltage. These sensors are used for controlling ...



Figure 13: The temperature sensors

Indeed, the data acquired from these sensors are sent to a DAQ card which processes these data with a PC, notably with LabView. Output signals from the Labview programs are also sent with this card (for example, to control the electro-valve).

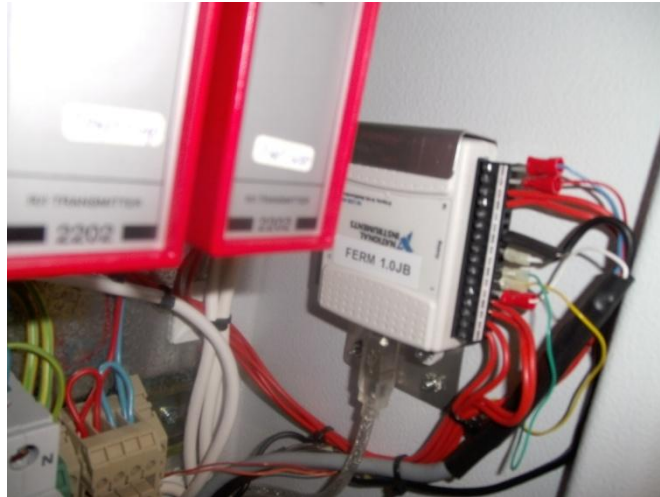


Figure 14: The DAQ card

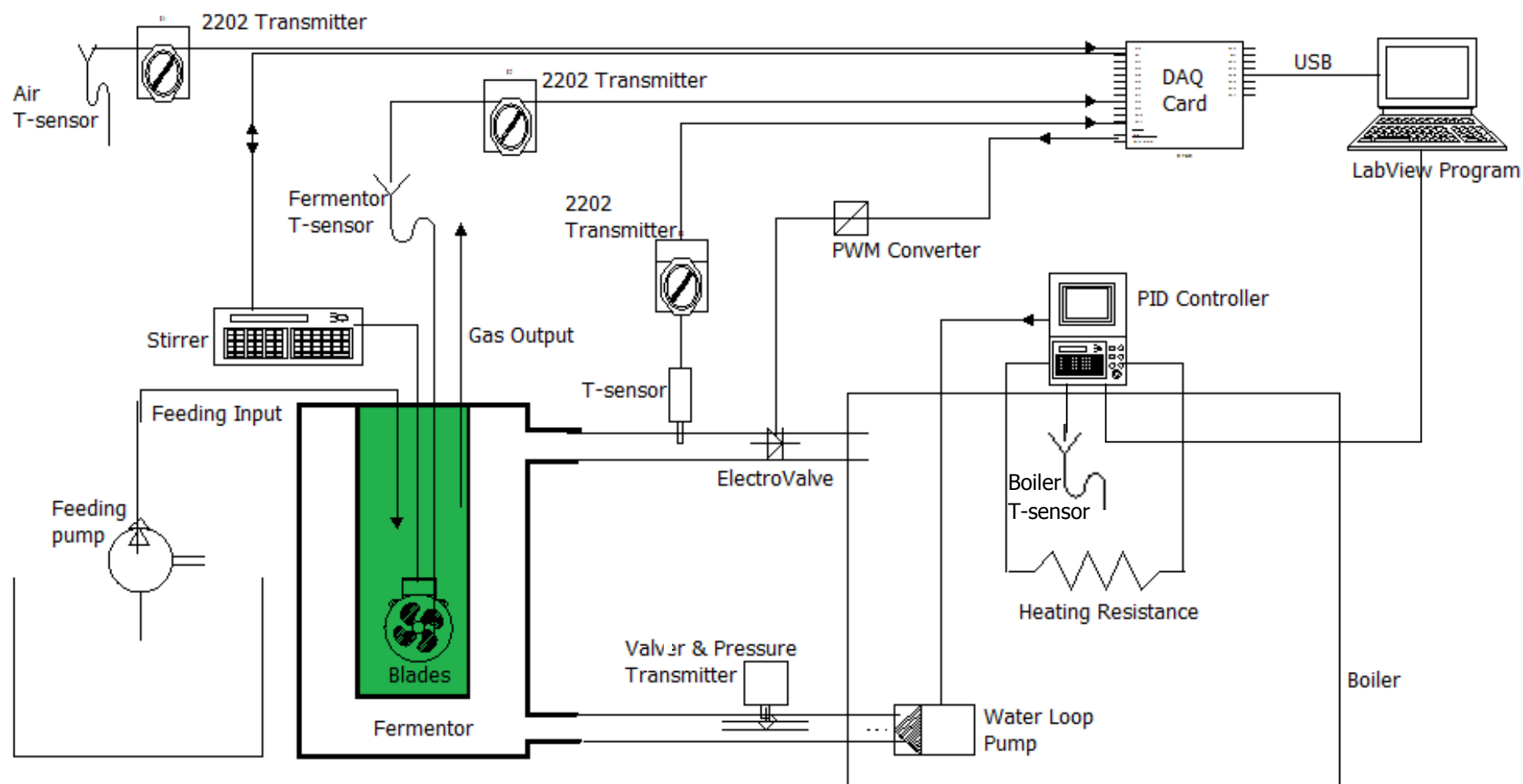


Figure 15 : The complete existing system

3. Problem Identification

3.1. The Existing Program

A LabView program to regulate the temperature and the stirring in the fermentor already exists. This program is able to regulate the temperature in the fermentor and the stirring speed from required setpoints (SP) entered by the user. It should also be able to follow the evolution of the process variables (PV) and the measured values (MV) as well as the temperature of the heating water.

A first step in this project has been to succeed in understanding and getting this program to work.

3.2. Objectives of the Thesis

The purpose of this project is to increase the energy efficiency and quickness of the control system by using an appropriate control and regulation strategy.

Analyzing the existing control program has determined the drawbacks of the strategy previously adopted. In this program, the temperature regulation is assured by the control of the electro-valve. It means that the heat transfer between the fermentor and the water loop is controlled by the water flow rate regulation.

This strategy presents several drawbacks from an energy point of view. First of all, at the water-pump level : when the electro-valve is partially open, the pump has to compensate for the pressure loss generated by the valve. The water flow rate is decreased while the energy provided by the pump to create this flow rate is the same as when the water flow rate is maximum.

Moreover, at the boiler level, only one operating temperature can be used in the boiler, 60°C in this case. This means that when the fermentor has to be cooled down (the reaction in the fermentor is exothermic), the boiler temperature is maintained at 60°C while the required temperature in the water loop is less. So, a energy loss is generated to compensate for the unavoidable losses to the ambient air.

Finally, several tests of the existing system reveal that the control implementation is far from perfect. Indeed, the valve tends to switch from totally open to totally closed and vice versa really quickly instead of finding an appropriate partial opening, to allow the correct heat transfer.

All these reasons led to the idea of the project, which is to control the temperature in the fermentor by acting on the boiler temperature (that is the boiler set point temperature) instead of acting on the electro-valve opening. So, the idea is to use a constant water flow rate and to regulate the amount of heat provided at the boiler level in order to control the fermentor temperature.

This strategy should increase the energy efficiency of the system because, first of all, no pressure losses are generated by a valve and, moreover, the energy provided by the boiler is regulated and no energy has to be provided when the fermentor has to be cooled down, for example.

Once the new program implemented, the evaluation result might reveal that a better result might be produced by using the both systems together (electro-valve control and boiler control).

4. Feasibility Analysis

4.1. Boiler Communication

In the strategy chosen for this project, a feed-back loop has to be implemented: the difference between the SP value and the PV value of the fermentor temperature has to be supplied to a new PID controller, implemented on LabView. The output of this new PID controller will constitute the temperature set point for the boiler. So, communication between the LabView program and the boiler's PID has to be implemented.

The boiler has a RS-232 input for serial communication. So, the communication between the computer and the boiler has been easily fulfilled using a simple a simple cross-over RS-232 cable.



Figure 16: The RS-232 connection

Moreover, the boiler constructor supplies useful Labview library (available in Annex 1) in order to easily control its equipment via LabView. This library includes VIs to initialize, configure, get data, manage errors and shut down the boiler. The library is used in this project to create Labview programs for testing the system and for implementing the solution.

That's how a Labview program has been created for test purpose. This program allows the user to choose a temperature for the boiler, to open or close the electro-

valve and to acquire data about the boiler and the various temperatures of the system.

4.2. Boiler Calibration

During the tests which follow, it was interesting and necessary to acquire the temperature values of the water at the input of the fermentor (called T_1 in the following paragraphs). Although no temperature sensor is present at this place in the water loop, the acquisition of this temperature has been possible thanks to the Absolute Temperature Calibration (ATC) function present with the boiler configuration. Indeed, this function allows the user to compensate for a difference that might occur between the circulator and a defined measuring point.

In this way, according to the temperature in the circulator (T_b) and the corresponding water temperature at the input of the fermentor (T_1), it is possible to configure the boiler to only take into account the value of T_1 instead of the value T_b . For other temperature values, an interpolation of the compensation is performed, according to the various calibrations points configured in the boiler by the user. Up to 3 calibration points can be configured in the boiler program.

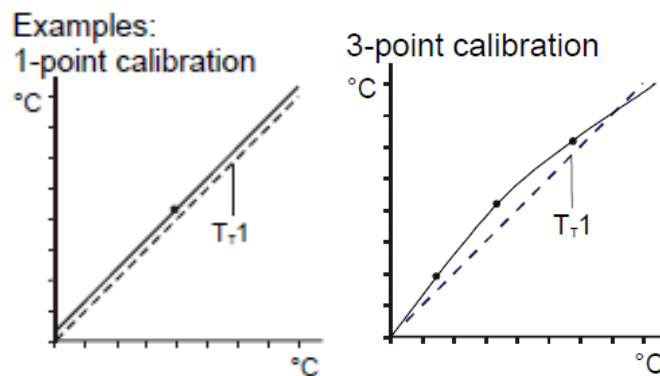


Figure 17 : Examples of temperature compensation of the boiler

In our case, two calibration points have been used : one point at 53°C, the operating temperature and one point at the ambient temperature, 23°C, which are the two temperatures used during the following tests. In the first case, T_1 has been measured as 51,2°C and in the second case, T_1 should be 23°C too because no losses with ambient air should occur. These two calibrations points entered in the

boiler, it is now possible to get (an approximate value of) T_1 from the serial communication with the boiler.

So, the relation between T_1 and T_b used by the ATC is :

$$T_1 = 0,94T_b + 1,38 \quad (1.1)$$

The approximation on T_1 should not be significant if we can consider the ambient temperature constant during the various tests ($T_a = 23^\circ C$ for each test).

5. Modeling the System

5.1. Introduction

Although a PID controller can be tuned with a trial-and error method, this way of working generally leads to poor results. Indeed :

"Many problems preclude the simple trial-and-error approach, on account of complexity, efficiency, cost or even danger. Also, a trial-and-error approach cannot answer before trial, questions such as :

- *[...] What controller can achieve the given objective ? Can it be achieved at all?*
- *How will the controller and the plant perform in closed loop?*
- *Why is the loop behaving the way it is ? Can it be done better? If so, by which controller ?*
- *How would the loop performance change if the system parameters were to change, or disturbances were larger, or a sensor to fail ?"*²

That's why a regulation project often depends on equations describing the system. This set of equations is called a model and allows *"capturing the behavior of the system in such a way that it can be manipulated outside the constraints of physical reality"*³

*"The power of a mathematical model lies in the fact that it can be simulated in hypothetical situations [...] and can be used as a basis for synthesizing controllers".*⁴

So, in the context of this project, an approximate mathematical model expressing the impact that control inputs (and disturbances, and initial conditions) have on the output will be set up.

The model in question is called "approximate" because such a model is often enough for regulation purpose. Indeed, a too precise model is too difficult to manipulate, while a too approximate model doesn't reflect the reality. The art of the control

² (GOODWIN, et al., 2001)

³ *Op. cit.*

⁴ *Op. cit.*

engineer is to elaborate a model in between these two extremes and to be able to estimate the errors involved with this approximate model.

In this project, the model is developed in several parts. First of all, the heat transfer between the water loop and the fermentor is modeled. Then the boiler behavior is modeled in its turn. Finally, the temperature losses occurring in the pipes are simulated.

5.2. First Fermentor Model

5.2.1. *Modeling the Fermentor*

Let's consider the system without any losses (fermentor and water loop perfectly insulated). We will also consider that the fermentor is full of reagents (volume occupied by the biogas product and by the air neglected).

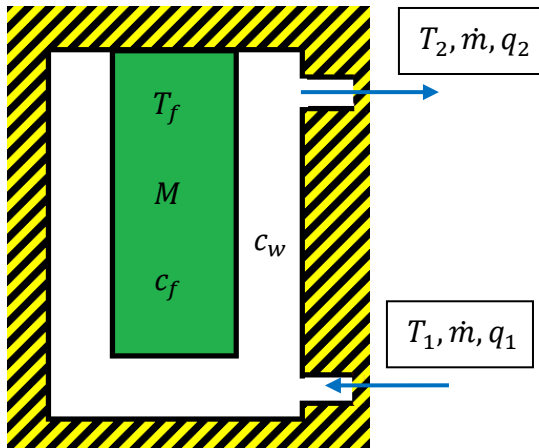


Figure 18 : The insulated fermentor

Let ...

$T_f[^\circ\text{C}]$: The temperature inside the fermentor (considered uniform because of the stirring).

$M[\text{kg}]$: The mass inside the fermentor

$c_f[\text{J.kg}^{-1}.^\circ\text{C}^{-1}]$: The specific heat capacity inside the fermentor

$c_w[\text{J.kg}^{-1}.^\circ\text{C}^{-1}]$: The specific heat capacity of the water

$\dot{m}[\text{kg/s}]$: The flow rate in the water loop

$T_1, T_2[^\circ\text{C}]$: The temperature of the water at the input and at the output of the fermentor

$q_1, q_2[\text{W}]$: The input and output rate of heat flow.

Let's try to express $T_f = f(T_1, t)$ where $t[\text{s}]$ is the time variable.

Considering the energy conservation law, we can say that the difference between the input and the output rate of heat flow is equal to the heat variation inside the fermentor : (Let Q [J] be the heat inside the fermentor)

$$q_1 - q_2 = \frac{dQ}{dt} \quad (1.2)$$

Thus, considering the specific heat capacity definition,

$$c_w \cdot \dot{m} \cdot (T_1 - T_2) = \frac{d(c_f \cdot M \cdot T_f)}{dt}$$

Since T_2 is a function of T_f , we have to write :

$$c_w \cdot \dot{m} \cdot (T_1 - T_2(T_f)) = c_f \cdot M \cdot \frac{dT_f}{dt} \quad (1.3)$$

which is a first-order differential equation with separated variables.

So, to continue, we have to find the $T_2 = f(T_f)$ expression.

Let's consider an infinitesimal height of the vessel :

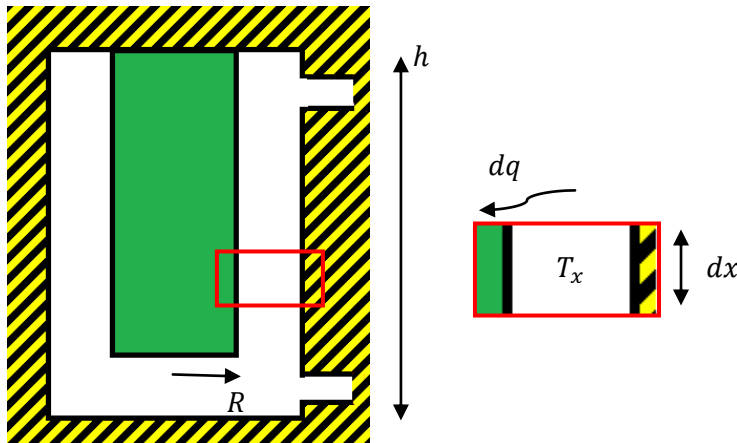


Figure 19: An infinitesimal height of the insulated fermentor

We have...

dx [m]: The height of the infinitesimal height.

T_x [K]: The temperature of the infinitesimal height

dq [W]: The rate of heat flow exchanged between the water and the fermentor in this infinitesimal height

R, h [m]: Dimensions of the fermentor

First of all, dq can be deduced by the specific heat capacity definition, considering the temperature difference between two neighboring infinitesimal heights, dT_x :

$$dq = -c_w \cdot \dot{m} \cdot dT_x \quad (1.4)$$

Besides, if we idealize the fluid mechanics of the water in the vessel, dq can also be deduced by fundamental relation of the heat exchangers⁵ :

$$dq = U(T_x - T_f) \cdot 2 \cdot \pi \cdot R \cdot dx$$

Where U [W/m²K] is the exchange coefficient leading the heat exchange between the water loop and the fermentor.

Combining these two equations, we have:

$$-c_w \cdot \dot{m} \cdot dT_x = U(T_x - T_f) \cdot 2 \cdot \pi \cdot R \cdot dx$$

$$\frac{-dT_x}{(T_x - T_f)} = \frac{U \cdot 2 \cdot \pi \cdot R \cdot dx}{c_w \cdot \dot{m}}$$

Considering U constant along the height of the fermentor :

$$\int_{T_1}^{T_2} \frac{dT_x}{(T_x - T_f)} = \frac{-U \cdot 2 \cdot \pi \cdot R}{c_w \cdot \dot{m}} \int_0^h dx$$

And considering $S = 2 \cdot \pi \cdot R \cdot h$, the exchange surface :

$$\ln\left(\frac{T_2 - T_f}{T_1 - T_f}\right) = \frac{-U \cdot S}{c_w \cdot \dot{m}}$$

$$T_2 = T_f + (T_1 - T_f) \cdot e^{\frac{-U \cdot S}{c_w \cdot \dot{m}}} \quad (1.5)$$

We can now use the expression of T_2 in the relation (1.3) :

$$c_w \cdot \dot{m} \cdot \left(T_1 - \left(T_f + (T_1 - T_f) \cdot e^{\frac{-U \cdot S}{c_w \cdot \dot{m}}} \right) \right) = c_f \cdot M \cdot \frac{dT_f}{dt} \quad (1.6)$$

Since this equation is a first-order differential equation with separated variables, it is quite easy to solve:

⁵ (KELNER, 2011)

$$\begin{aligned}
\frac{c_w \cdot \dot{m}}{c_f \cdot M} \cdot dt &= \frac{d(T_f)}{T_1 - \left(T_f + (T_1 - T_f) \cdot e^{\frac{-U \cdot S}{c_w \cdot \dot{m}}} \right)} \\
\frac{c_w \cdot \dot{m}}{c_f \cdot M} \cdot dt &= \frac{d(T_f)}{\left(1 - e^{\frac{-U \cdot S}{c_w \cdot \dot{m}}} \right) \cdot (T_1 - T_f)} \\
\frac{c_w \cdot \dot{m}}{c_f \cdot M} \cdot \int_0^t dt &= - \int_{T_{f0}}^{T_f(t)} \frac{d(T_f)}{\left(1 - e^{\frac{-U \cdot S}{c_w \cdot \dot{m}}} \right) \cdot (T_f - T_1)} \\
\frac{c_w \cdot \dot{m}}{c_f \cdot M} \cdot \left(1 - e^{\frac{-U \cdot S}{c_w \cdot \dot{m}}} \right) \cdot t &= - \ln \left(\frac{(T_f(t) - T_1)}{(T_{f0} - T_1)} \right) \\
T_f(t, T_1) &= T_1 + (T_{f0} - T_1) \cdot e^{\frac{-c_w \cdot \dot{m}}{c_f \cdot M} \cdot \left(1 - e^{\frac{-U \cdot S}{c_w \cdot \dot{m}}} \right) \cdot t} \quad (1.7)
\end{aligned}$$

This expression lets us predict the evolution of T_f with time, according to the value of T_1 and to T_{f0} , the initial value of T_f .

The parameters to determine in order to use this expression are: M , c_f , c_w , \dot{m} , U , S .

It's important to remember that this expression relies on several hypotheses:

- Perfectly insulated fermentor;
- Uniform temperature in the fermentor (because of the stirring).
- Fermentor full of reagents.
- Idealized fluid mechanic of the water in the vessel (one dimension motion according to the x axis).
- Inferior circular exchange surface neglected.
- U considered as constant along the fermentor.

5.2.2. *Determining the parameters for the fermentor demonstration system*

Direct parameters :

In order to verify the model, we can operate a test and compare the temperature measurements with the result expected with the model's formulae. To achieve this, we need to determine the multiple parameters of the formula:

M : Depending on test conditions, in our case 3,5kg

c_w : We will use the value of 4182 [J.kg⁻¹.°C⁻¹], which is the value for water at 53°C but also at 20°C. ⁶

c_f : For demonstration test purpose, the material used in the fermentor to analyze heat transfer is water. So, 4182 [J.kg⁻¹.°C⁻¹]

\dot{m} : The water flow rate has been measured by opening the water loop at the end of the loop (that is at the input of the boiler). Three measurements have been taken, which lead to the following value for the water flow rate :

$$\begin{array}{r} 1 \quad 0,9[\text{kg}]/42,94[\text{s}] \\ 2 \quad 0,9[\text{kg}]/45,16[\text{s}] \\ 3 \quad 0,9[\text{kg}]/44,14[\text{s}] \\ \hline 0,9[\text{kg}]/44,08[\text{s}] \\ = \mathbf{0,02042 \text{ [kg/s]}} \end{array}$$

S : In the model, only the vertical cylindrical surface was considered. However, heat transfer also takes place in the inferior circular surface (base of the cylinder). Thus, we can add this area to the area in consideration. So, the approximate exchange surface is equivalent to a vertical cylindrical surface with a bigger radius.

$$S = 2.\pi.R.h + \pi.R^2 = 2.\pi.0,08.0,28 + \pi.0,08^2 = 0,14533 \text{ m}^2$$

⁶ (MESSE, 2002)

Determining U :

U is the hardest parameter to define. This parameter defines the rate of heat exchanged between the water loop and the fermentor. In order to determine U , a test has been established. Because of the hypothesis on which the model is based, the temperature of the water loop has been set to the ambient temperature (T_a), so that the losses can be neglected, as the model requires. The initial value of T_f could be set higher or lower than this temperature. A Labview program has been created in order to acquire and compute the evolutions of T_f , T_1 and T_2 in the time. Here are examples of the evolution of these temperatures within time (values in °C, time in seconds):

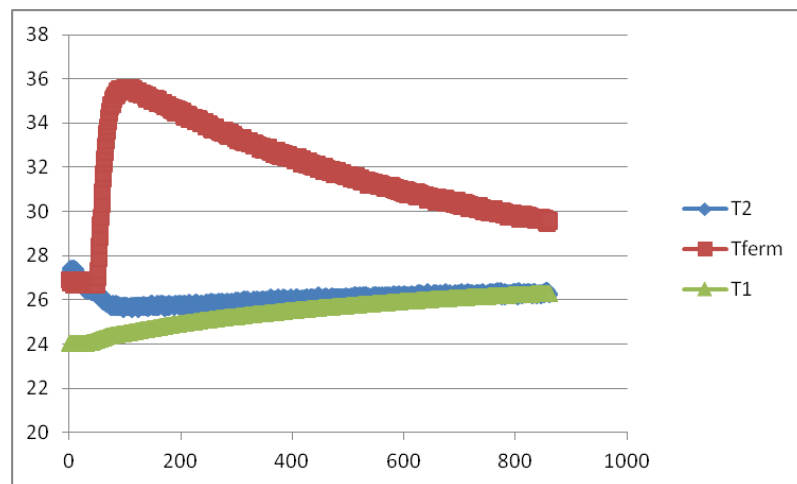


Figure 20 : Test at ambient temperature ($T_a = 25,5^\circ\text{C}$) and warmer fermentor

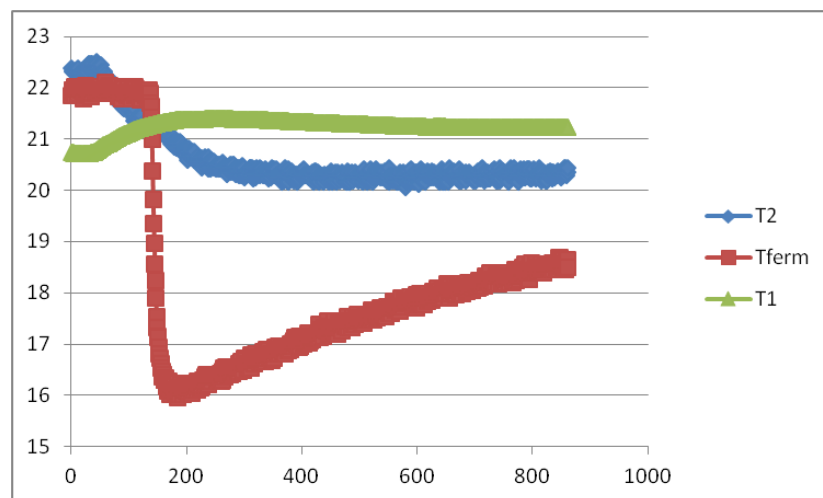


Figure 21 : Test at ambient temperature ($T_a = 21,2^\circ\text{C}$) and colder fermentor

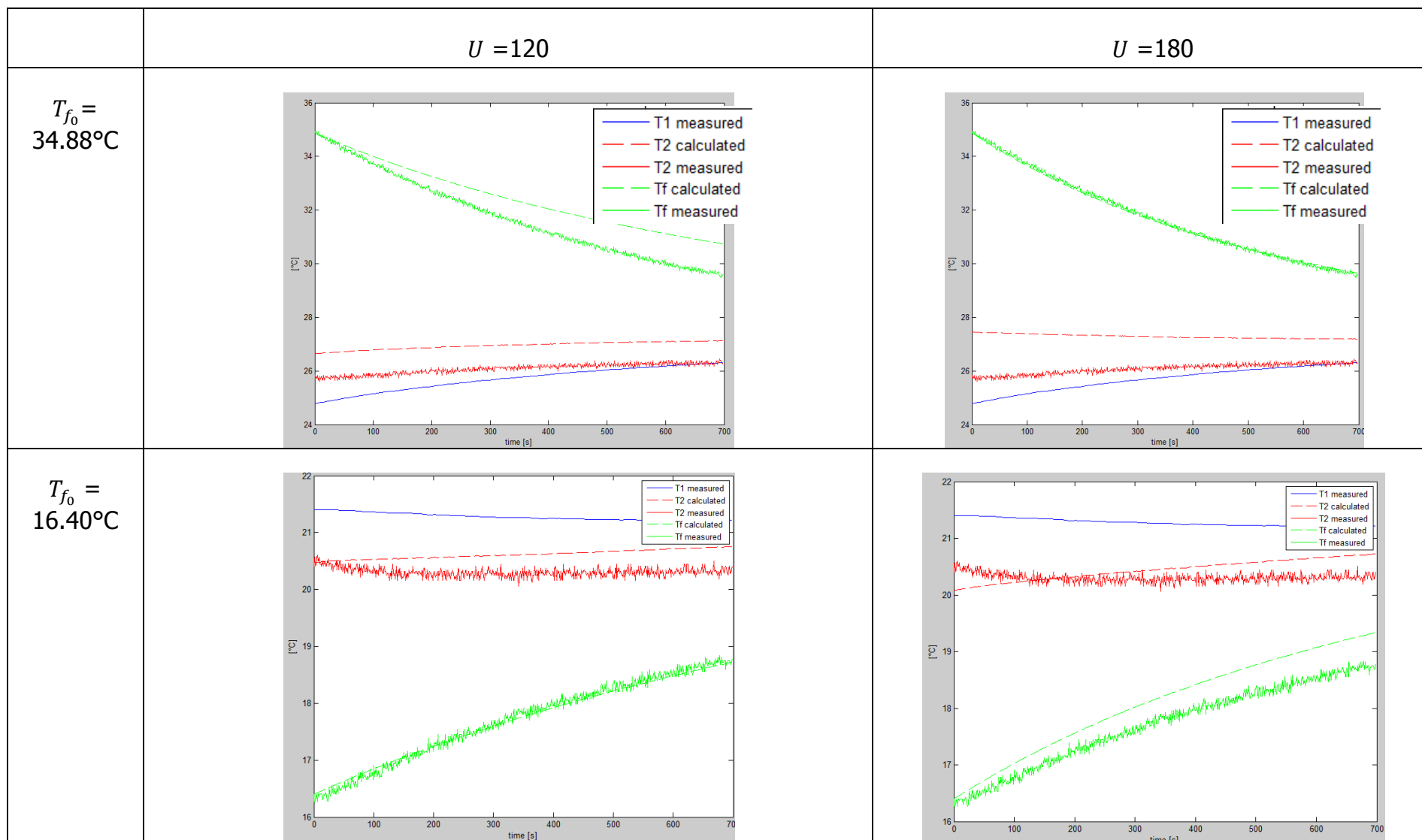
A first attempt to determine U consisted in determining U using the formula (1.5) or (1.7) :

$$U = -\frac{c_w \cdot \dot{m}}{S} \cdot \ln\left(\frac{T_2 - T_f}{(T_1 - T_f)}\right)$$

$$U = -\frac{c_w \cdot \dot{m}}{S} \cdot \ln\left(\frac{c_f \cdot M}{c_w \cdot \dot{m} \cdot t} \cdot \ln\left(\frac{T_f - T_1}{(T_{f0} - T_1)}\right) + 1\right)$$

A second attempt consisted in calculating the evolution of T_2 and T_f according to the formulae (1.5) and (1.7) respectively and to the measured values of T_1 . After that, these calculated values of T_2 and T_f were compared with the measured values of T_2 and T_f . Using a MATLAB script to compare these values allowed adjusting the value of U in order to fit the T_f calculated values with the T_f measured values.

Unfortunately, neither of these two attempts delivered reliable results. Indeed, the first attempt leads to non-constant values of U with time and the second attempt doesn't lead to the same value of U when different initial values of T_f are considered. The following graphs show the problem:



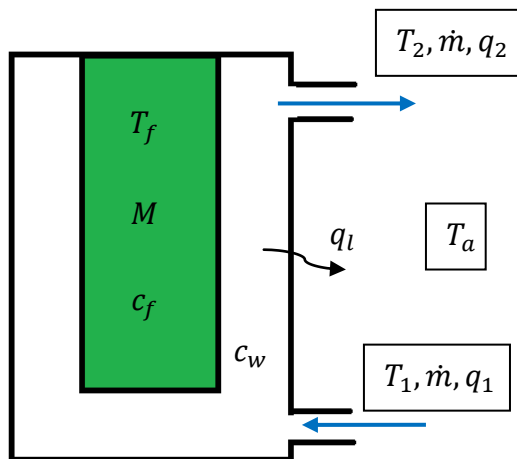
The reason for this failure is that the value of U depends on the different temperatures T_x and on T_f . Thus, different tests executed with different temperatures lead to different values of U . The explanation of this phenomenon can be understood by reading the *VDI Heat Atlas, Section C2* mentioned in the bibliography⁷. The heat transfer occurring in the fermentor is a mixture of conduction and forced convection.

That's why, for a control aim, it is necessary to determine U around the normal steady state operating point of the fermentor, that is 53°C. However, such a temperature will cause losses to the ambient air that's why the hypothesis of a perfectly insulated fermentor can't be maintained. So, it is necessary to improve the previous model by taking into account the losses generated because of the non-insulated fermentor...

5.3. Second Fermentor Model

5.3.1. *Modeling the Losses*

Let's consider the same system as previously, but taking the losses into account...



Let's add the following variables:

q_l [W]: The rate of heat flow lost because of the ambient air

T_a [K] : The temperature of the ambient air

Figure 22: The fermentor

Now, the equation (1.2) has to consider this energy loss :

⁷ (ROETZEL, et al., 2010)

$$q_1 - q_2 = \frac{dQ}{dt} + q_l$$

$$c_w \cdot \dot{m} \cdot (T_1 - T_2(T_f)) = c_f \cdot M \cdot \frac{dT_f}{dt} + q_l \quad (1.8)$$

To solve this equation, we have to find the $T_2 = f(T_f)$ expression but also the expression of q_l .

In order to achieve these two requirements, let's consider the infinitesimal height of the vessel again:

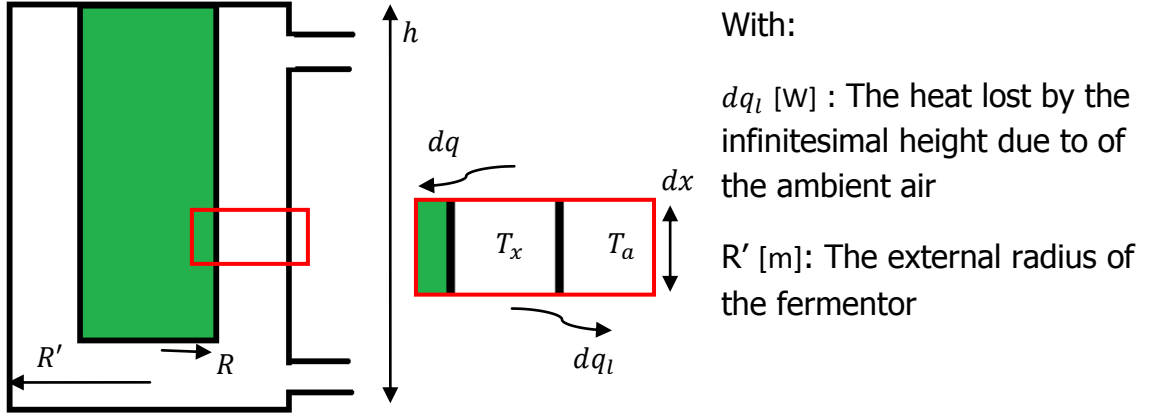


Figure 23: An infinitesimal height of the fermentor

The equation (1.4) of the first model has to take the dq_l term into account:

$$dq + dq_l = -c_w \cdot \dot{m} \cdot dT_x \quad (1.9)$$

With

$$dq = U(T_x - T_f) \cdot 2 \cdot \pi \cdot R \cdot dx \quad (1.10)$$

And

$$dq_l = U'(T_x - T_a) \cdot 2 \cdot \pi \cdot R' \cdot dx \quad (1.11)$$

Where U' [W/m²/°C] is the exchange coefficient leading the heat exchange between the air and the water loop.

Integrating this previous equation allows us to determine q_l :

$$\int_0^{q_l} dq_l = \int_0^h U'(T_x(x) - T_a). 2. \pi. R'. dx$$

$$q_l = -U'. T_a. S' + U'. 2. \pi. R' \int_0^h T_x(x) dx \quad (1.12)$$

with $S' = 2. \pi. R'. h$, the external exchange surface.

We now have to determine the $T_x = f(x)$ expression. It can be done by combining the equations (1.9), (1.10) et (1.11) :

$$- c_w. \dot{m}. dT_x = U(T_x - T_f). 2. \pi. R. dx + U'(T_x - T_a). 2. \pi. R'. dx$$

$$- c_w. \dot{m}. dT_x = 2\pi (T_x(U. R + U'. R') - (U. R. T_f + U'. R'. T_a)) dx \quad (1.13)$$

$$- \frac{c_w. \dot{m}}{(U. R + U'. R')} \cdot \int_{T_1}^{T_x} \frac{dT_x}{T_x - \frac{(U. R. T_f + U'. R'. T_a)}{(U. R + U'. R')}} = 2\pi \int_0^x dx$$

$$\ln \left(\frac{T_x - \frac{(U. R. T_f + U'. R'. T_a)}{(U. R + U'. R')}}{T_1 - \frac{(U. R. T_f + U'. R'. T_a)}{(U. R + U'. R')}} \right) = -2. \pi. x. \frac{(U. R + U'. R')}{c_w. \dot{m}}$$

$$T_x = \frac{(U. R. T_f + U'. R'. T_a)}{(U. R + U'. R')} + \left(T_1 - \frac{(U. R. T_f + U'. R'. T_a)}{(U. R + U'. R')} \right) e^{-2. \pi. x. \frac{(U. R + U'. R')}{c_w. \dot{m}}}$$

This expression of T_x can now be used in the equation (1.12) :

$$q_l = -U'. T_a. S'$$

$$+ U'. 2. \pi. R' \int_0^h \frac{(U. R. T_f + U'. R'. T_a)}{(U. R + U'. R')} dx$$

$$+ \left(T_1 - \frac{(U. R. T_f + U'. R'. T_a)}{(U. R + U'. R')} \right) e^{-2. \pi. x. \frac{(U. R + U'. R')}{c_w. \dot{m}}} dx$$

$$q_l = -U'.T_a.S' + U'.S'.\left(\frac{(U.R.T_f + U'.R'.T_a)}{(U.R + U'.R')}\right) + U'.2.\pi.R'.\left(T_1 - \frac{(U.R.T_f + U'.R'.T_a)}{(U.R + U'.R')}\right) \cdot \frac{e^{-2.\pi.h.\frac{(U.R+U'.R')}{c_w.\dot{m}}} - 1}{-2.\pi.\frac{(U.R + U'.R')}{c_w.\dot{m}}}$$

Finally, the expression $T_2 = f(T_f)$ can be deduced from the equation (1.13) by integrating on the complete height of the fermentor :

$$-\frac{c_w.\dot{m}}{(U.R + U'.R')} \cdot \int_{T_1}^{T_2} \frac{dT_x}{T_x - \frac{(U.R.T_f + U'.R'.T_a)}{(U.R + U'.R')}} = 2\pi \int_0^h dx$$

This equation leads to the following result :

$$T_2 = \frac{(U.R.T_f + U'.R'.T_a)}{(U.R + U'.R')} + \left(T_1 - \frac{(U.R.T_f + U'.R'.T_a)}{(U.R + U'.R')}\right) e^{-2.\pi.h.\frac{(U.R+U'.R')}{c_w.\dot{m}}} \quad (1.14)$$

Writing the function $a(T_f, Ta) = \frac{(U.R.T_f + U'.R'.T_a)}{(U.R + U'.R')}$ and the variable $b = \frac{-2.\pi.(U.R+U'.R')}{c_w.\dot{m}}$, the expressions of q_l and T_2 become:

$$q_l = -U'.T_a.S' + U'.S'.a(T_f, Ta) + U'.2.\pi.R'.(T_1 - a(T_f, Ta)) \cdot \frac{e^{h.b} - 1}{b}$$

$$T_2 = a(T_f, Ta) + (T_1 - a(T_f, Ta)) e^{h.b}$$

Combining these two expressions with (1.8), we find the differential equation defining the evolution of T_f according to T_1 and:

$$\begin{aligned}
& c_w \cdot \dot{m} \cdot (T_1 - (a(T_f, Ta) + (T_1 - a(T_f, Ta)) e^{h.b})) \\
&= c_f \cdot M \cdot \frac{dT_f}{dt} - U' \cdot T_a \cdot S' + U' \cdot S' \cdot a(T_f, Ta) \\
&+ U' \cdot 2 \cdot \pi \cdot R' \cdot (T_1 - a(T_f, Ta)) \cdot \frac{e^{h.b} - 1}{b} \\
& c_w \cdot \dot{m} \cdot (1 - e^{h.b}) \cdot (T_1 - a(T_f, Ta)) \\
&= c_f \cdot M \cdot \frac{dT_f}{dt} - S' \cdot U' \cdot T_a + U' \cdot S' \cdot a(T_f, Ta) \\
&- U' \cdot 2 \cdot \pi \cdot R' \cdot \frac{1 - e^{h.b}}{b} \cdot (T_1 - a(T_f, Ta)) \\
& \left(c_w \cdot \dot{m} + \frac{U' \cdot 2 \cdot \pi \cdot R'}{b} \right) \cdot (1 - e^{h.b}) \cdot (T_1 - a(T_f, Ta)) \\
&= c_f \cdot M \cdot \frac{dT_f}{dt} + U' \cdot S' \cdot (a(T_f, Ta) - T_a)
\end{aligned} \tag{1.15}$$

This equation is also a first-order differential equation with separable variables and can be easily solved by separating the variables and integrating each term of the equation. However, mathematics provides us with a powerful tool, useful in analyzing the system without solving the differential equations: the Laplace Transform.

This mathematical tool is particularly famous in control engineering because it converts differential equations into algebraic equations, easier to manipulate. These algebraic equations lead to the definition of a so called "transfer function" which characterizes the system.

5.3.2. Identification of the fermentor transfer function

The transfer function of the system can be deduced from the differential equation defining the system, the equation (1.15).

Once simplified, we have,

$$\begin{aligned}
c_f \cdot M \cdot \frac{dT_f}{dt} &= \left(c_w \cdot \dot{m} + \frac{U' \cdot 2 \cdot \pi \cdot R'}{b} \right) \cdot (1 - e^{h.b}) \cdot (T_1 - a(T_f, Ta)) \\
&- U' \cdot S' \cdot (a(T_f, Ta) - T_a)
\end{aligned}$$

Applying the Laplace Transform :

$$c_f.M. \mathcal{L}\left[\frac{dT_f}{dt}\right] = \left(c_w.\dot{m} + \frac{U'.2.\pi.R'}{b}\right). (1 - e^{h.b}). \mathcal{L}[T_1 - a(T_f, Ta)] \\ - U'.S'. \mathcal{L}[a(T_f, Ta) - Ta]$$

Considering that ...

$$\mathcal{L}[a(T_f, Ta)] = \frac{UR \mathcal{T}_f(s) + U'R' \mathcal{T}_a(s)}{UR + U'R'}$$

we obtain:

$$c_f.M.s. \mathcal{T}_f(s) - T_{f_0} \\ = \left(c_w.\dot{m} + \frac{U'.2.\pi.R'}{b}\right). (1 - e^{h.b}). \left(\mathcal{T}_1(s) - \frac{UR \mathcal{T}_f(s) + U'R' \mathcal{T}_a(s)}{UR + U'R'}\right) \\ - U'.S'. \left(\frac{UR \mathcal{T}_f(s) + U'R' \mathcal{T}_a(s)}{UR + U'R'} - \mathcal{T}_a(s)\right) \quad (1.16)$$

And considering a zero initial condition,

$$c_f.M.s. \mathcal{T}_f(s) = \left(c_w.\dot{m} + \frac{U'.2.\pi.R'}{b}\right). (1 - e^{h.b}). \left(\mathcal{T}_1(s) - \frac{UR \mathcal{T}_f(s) + U'R' \mathcal{T}_a(s)}{UR + U'R'}\right) \\ - U'.S'. \left(\frac{UR \mathcal{T}_f(s) + U'R' \mathcal{T}_a(s)}{UR + U'R'} - \mathcal{T}_a(s)\right)$$

We can observe that the output T_f is generated by two distinct outputs T_1 and T_a . The superposition principle indicates that the response produced by the sum of two signals is equal to the sum of the responses to separate each signal⁸.

So, the two following schemes are equivalent:



Figure 24: Control scheme of the fermentor

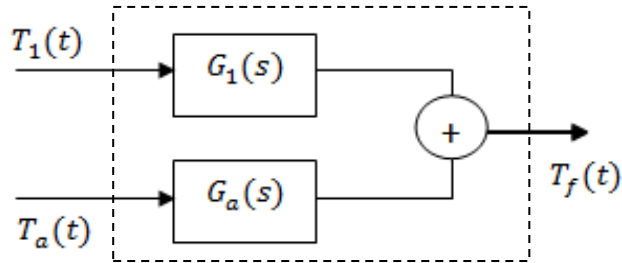


Figure 25 : Control scheme of the fermentor with separate signals

We can define the transfer functions $G_1(s)$ and $G_a(s)$ by cancelling out respectively the terms $\mathcal{T}_a(s)$ and $\mathcal{T}_1(s)$ in the previous expression.

Calculating $G_1(s)$:

Cancelling out $\mathcal{T}_a(s)$ in the previous expression:

$$c_f.M.s.\mathcal{T}_f(s) = \left(c_w.\dot{m} + \frac{U'.2.\pi.R'}{b} \right) . (1 - e^{h.b}) . \left(\mathcal{T}_1(s) - \frac{UR\mathcal{T}_f(s)}{UR + U'R'} \right) - U'.S'. \left(\frac{UR\mathcal{T}_f(s)}{UR + U'R'} \right)$$

the transfer function $G_1(s)$ can now be identified:

⁸ (VETCOUR, 2011-2012)

$$\begin{aligned}
\mathcal{T}_f(s) & \left[c_f.M.s + \frac{U'S'UR}{UR + U'R'} + \frac{UR}{UR + U'R'} \cdot \left(c_w.\dot{m} + \frac{U'.2.\pi.R'}{b} \right) \cdot (1 - e^{h.b}) \right] \\
& = \left[\left(c_w.\dot{m} + \frac{U'.2.\pi.R'}{b} \right) \cdot (1 - e^{h.b}) \right] \mathcal{T}_1(s) \\
G_1(s) & = \frac{\mathcal{T}_f(s)}{\mathcal{T}_1(s)} = \frac{\left(c_w.\dot{m} + \frac{U'.2.\pi.R'}{b} \right) \cdot (1 - e^{h.b})}{c_f.M.s + \frac{U'S'UR}{UR + U'R'} + \frac{UR}{UR + U'R'} \cdot \left(c_w.\dot{m} + \frac{U'.2.\pi.R'}{b} \right) \cdot (1 - e^{h.b})}
\end{aligned}$$

Stating the factors

$$K_1 = \frac{\left(c_w.\dot{m} + \frac{U'.2.\pi.R'}{b} \right) \cdot (1 - e^{h.b})}{c_f.M} \quad (1.17)$$

and

$$p_1 = - \frac{\frac{U'S'UR}{UR + U'R'} + \frac{UR}{UR + U'R'} \cdot \left(c_w.\dot{m} + \frac{U'.2.\pi.R'}{b} \right) \cdot (1 - e^{h.b})}{c_f.M} \quad (1.18)$$

We can now write the Evan's form of the transfer function, where K_1 and p_1 are the static gain and the pole of the transfer function, respectively:

$$G_1(s) = \frac{K_1}{s - p_1}$$

Calculating $G_a(s)$:

This time, we have to cancel out $\mathcal{T}_1(s)$:

$$\begin{aligned}
c_f.M.s.\mathcal{T}_f(s) & = \left(c_w.\dot{m} + \frac{U'.2.\pi.R'}{b} \right) \cdot (1 - e^{h.b}) \cdot \left(- \frac{UR\mathcal{T}_f(s) + U'R'\mathcal{T}_a(s)}{UR + U'R'} \right) \\
& \quad - U'.S' \cdot \left(\frac{UR\mathcal{T}_f(s) + U'R'\mathcal{T}_a(s)}{UR + U'R'} - \mathcal{T}_a(s) \right)
\end{aligned}$$

The transfer function $G_1(s)$ can now be identified :

$$\begin{aligned}
\mathcal{T}_f(s) & \left[c_f.M.s + \frac{U'S'UR}{UR + U'R'} + \frac{UR}{UR + U'R'} \cdot \left(c_w.\dot{m} + \frac{U'.2.\pi.R'}{b} \right) \cdot (1 - e^{h.b}) \right] \\
& = \mathcal{T}_a(s) \left[\left(c_w.\dot{m} + \frac{U'.2.\pi.R'}{b} \right) \cdot (1 - e^{h.b}) \cdot \frac{-U'R'}{UR + U'R'} - \frac{U'S'U'R'}{UR + U'R'} \right. \\
& \quad \left. + U'S' \right] \\
G_a(s) & = \frac{\mathcal{T}_f(s)}{\mathcal{T}_a(s)} = \frac{\left[\left(c_w.\dot{m} + \frac{U'.2.\pi.R'}{b} \right) \cdot (1 - e^{h.b}) \cdot \frac{-U'R'}{UR + U'R'} - \frac{U'S'U'R'}{UR + U'R'} + U'S' \right]}{c_f.M.s + \frac{U'S'UR}{UR + U'R'} + \frac{UR}{UR + U'R'} \cdot \left(c_w.\dot{m} + \frac{U'.2.\pi.R'}{b} \right) \cdot (1 - e^{h.b})}
\end{aligned}$$

Stating the factors

$$K_a = \frac{\left(c_w.\dot{m} + \frac{U'.2.\pi.R'}{b} \right) \cdot (1 - e^{h.b}) \cdot \frac{-U'R'}{UR + U'R'} - \frac{U'S'U'R'}{UR + U'R'} + U'S'}{c_f.M} \quad (1.19)$$

and

$$p_a = - \frac{\frac{U'S'UR}{UR + U'R'} + \frac{UR}{UR + U'R'} \cdot \left(c_w.\dot{m} + \frac{U'.2.\pi.R'}{b} \right) \cdot (1 - e^{h.b})}{c_f.M}$$

We can now write the Evan's form of the transfer function, where K_1 and p_1 are the static gain and the pole of the transfer function, respectively :

$$G_a(s) = \frac{K_a}{s - p_a}$$

Let's note that $p_a = p_1 (= p)$

Linear State Space Model :

According to the *Control System Design* reference book, "A very valuable and frequently used tool for plant modeling is a state-variable description,[...] the general form of which is : " ⁹

⁹ (GOODWIN, et al., 2001)

$$\frac{dx}{dt} = f(x(t), u(t), t)$$

$$y(t) = g(x(t), u(t), t)$$

Where $x(t)$ is the vector corresponding to a particular choice of state variable, $u(t)$ is the inputs vector and $y(t)$ the outputs vector.

"In the linear, time-invariant case, both equations become :"¹⁰

$$\frac{dx}{dt} = \mathbf{A}x(t) + \mathbf{B}u(t) \quad (1.20)$$

$$y(t) = \mathbf{C}x(t) + \mathbf{D}u(t) \quad (1.21)$$

The model is then called "*Linear State Space Model*"

Besides, it appears that the system described in our model matches with this definition. Indeed, we can rearrange the equation (1.15) in this way :

$$\frac{dT_f}{dt} = k_1 \cdot T_1 + k_f \cdot T_f + k_a \cdot T_a \quad (1.22)$$

Where

$$k_1 = \frac{\left(c_w \cdot \dot{m} + \frac{U' \cdot 2 \cdot \pi \cdot R'}{b} \right) \cdot (1 - e^{h \cdot b})}{c_f \cdot M}$$

$$k_f = \frac{\left(c_w \cdot \dot{m} + \frac{U' \cdot 2 \cdot \pi \cdot R'}{b} \right) \cdot (1 - e^{h \cdot b}) \cdot \frac{-UR}{UR + U'R'} - \frac{U'S'U'R'}{UR + U'R'}}{c_f \cdot M}$$

$$k_a = \frac{\left(c_w \cdot \dot{m} + \frac{U' \cdot 2 \cdot \pi \cdot R'}{b} \right) \cdot (1 - e^{h \cdot b}) \cdot \frac{-U'R'}{UR + U'R'} - \frac{U'S'U'R'}{UR + U'R'} + U'S'}{c_f \cdot M}$$

We can now see that the model is a Linear State Space Model by taking :

¹⁰ *Op. cit.*

$$x = y = T_f ; u = \begin{bmatrix} T_1 \\ T_a \end{bmatrix} ; A = k_f ; B = [k_1 \quad k_a] ; C = 1 ; D = 0$$

Indeed, in this case, equations (1.20) and (1.21) describe (1.22).

The transfer function of a Linear State Space Model is given in the reference book¹¹ by the formula:

$$G(s) = C(sI - A)^{-1}B + D \quad (1.23)$$

In our case :

$$G(s) = \begin{bmatrix} \frac{k_1}{s - k_f} & \frac{k_a}{s - k_f} \end{bmatrix} = [G_1(s) \quad G_a(s)]$$

And the scheme of the model becomes :

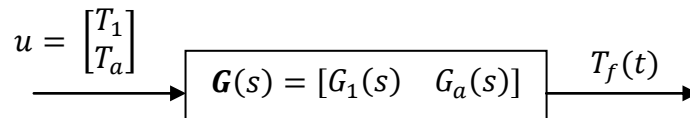


Figure 26: Control scheme of the fermentor, matrix point of view.

which is equivalent to the scheme of Figure 25.

5.3.3. Remembering the hypotheses

Let's remember the hypotheses established and let's note the new hypotheses of this second model :

- Uniform temperature in the fermentor (because of the stirring).
- Fermentor full of reagents.
- Idealized fluid mechanic of the water in the vessel (one dimension motion according to the x axis).
- Inferior circular exchange surface neglected.
- U considered as constant along the fermentor.
- Heat losses from the top and bottom of the fermentor is omitted

¹¹ (GOODWIN, et al., 2001)

- During tests with the demonstration system (water used as material in the fermentor), evaporation of the material in the fermentor omitted.

5.3.4. *Determining the parameters of the transfer function*

We see that the transfer function depends on the following parameters:

$c_w, c_f, M, \dot{m}, U, U', R, R', S, S', h$.

M, c_f, c_w, \dot{m}, S have already been determinate in 5.2.2 . Let's try to determine the other ones...

Determining R', S', h :

h : 0,28m

R : According to what is said about the determination of S , the value of R will be the radius of the equivalent vertical cylindrical surface with a value of area S :

$$R = \frac{S}{2 \cdot \pi \cdot h} = \frac{0,14533}{2 \cdot \pi \cdot 0,28} = 0,0826 \text{ m}$$

S' : It is determined in the same way as S , but here, both bases of the cylinder have to be taken into account :

$$S' = 2 \cdot \pi \cdot R' \cdot h + 2 \cdot \pi \cdot R'^2 = 2 \cdot \pi \cdot 0,09 \cdot 0,28 + 2 \cdot \pi \cdot 0,09^2 = 0,20923 \text{ m}^2$$

R' : It is determined in the same way:

$$R' = \frac{S'}{2 \cdot \pi \cdot h} = \frac{0,20923}{2 \cdot \pi \cdot 0,28} = 0,1189$$

Determining U, U' :

These two parameters can't be determined separately, or at least not easily. Indeed, in a test, these parameters are determined by the evolutions of temperatures. However, temperatures depend on the heat exchange between the fermentor and the water loop and on the heat exchange between the water loop and the ambient

air, that is U and U' at the same time. At 53°C, it is not possible to get temperatures varying only due to one of these two aspects.

That's why we will try to determine the transfer function in the following way, with the help of MatLab...

When the transfer function $G(s)$ is known, it is possible to find $T_f = f(T_1(t), T_a(t))$. So, during a test, we will measure and compute the evolution of T_f , T_1 and T_a .

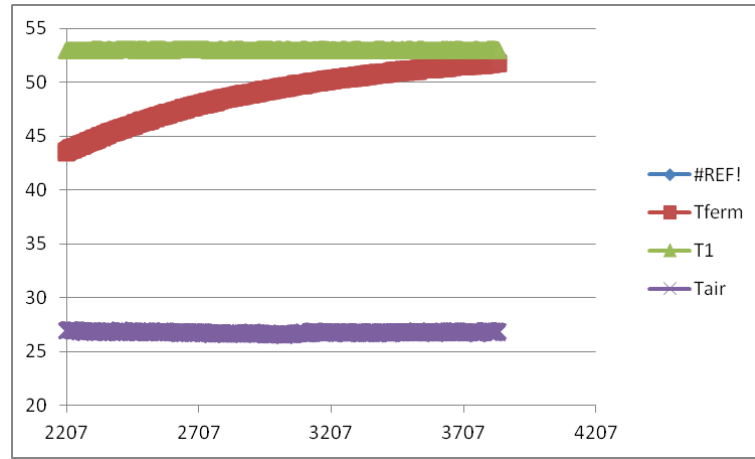


Figure 27 : Measures acquired during the test

Then in MatLab, we will try to find the pair (U, U') in order to fit the calculated value $T_f = f(T_1(t), T_a(t))$ with the measured value of T_f .

The function $T_f = f(T_1(t), T_a(t))$ is deduced as follows:

From the scheme of the transfer function, we know that

$$\mathcal{T}_f(s) = G_1(s) \cdot \mathcal{T}_1(s) + G_a(s) \cdot \mathcal{T}_a(s) + \frac{T_{f_0}}{s - p}$$

Applying the inverse Laplace Transform :

$$T_f(t) = \int_0^t g_1(\tau) \cdot T_1(t - \tau) d\tau + \int_0^t g_a(\tau) \cdot T_a(t - \tau) d\tau + T_{f_0} \cdot e^{pt}$$

where

$$g_1(t) = \mathcal{L}^{-1}(G_1) = \mathcal{L}^{-1}\left(\frac{K_1}{s - p_1}\right) = K_1 \cdot e^{pt} \text{ and } g_a(t) = K_a \cdot e^{pt}$$

During the test, measurements revealed that $T_1(t)$ and $T_a(t)$ can be considered as constants. So,

$$T_f(t) = T_{f_0} \cdot e^{pt} + (K_1 \cdot T_1 + K_a \cdot T_a) \frac{e^{pt} - 1}{p} \quad (1.24)$$

where K_1 , K_a and p depend on U and U' .

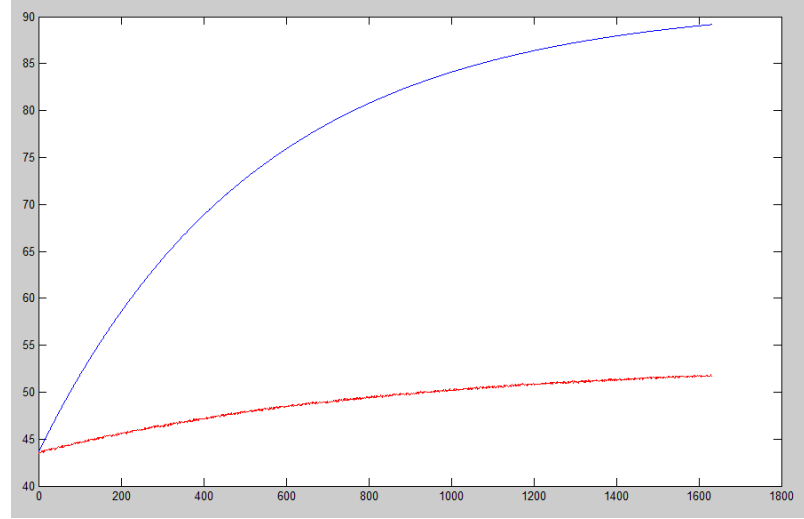


Figure 28: Example of the measured value (in red) and of the calculated value (in blue) of T_f , for $U=200$ and $U'=100$

To find the value of U and U' , the optimization tool of MatLab, *optimtool* has been tried. But this method didn't provide good results, probably because of a lack of knowledge in the field of optimization from the user.

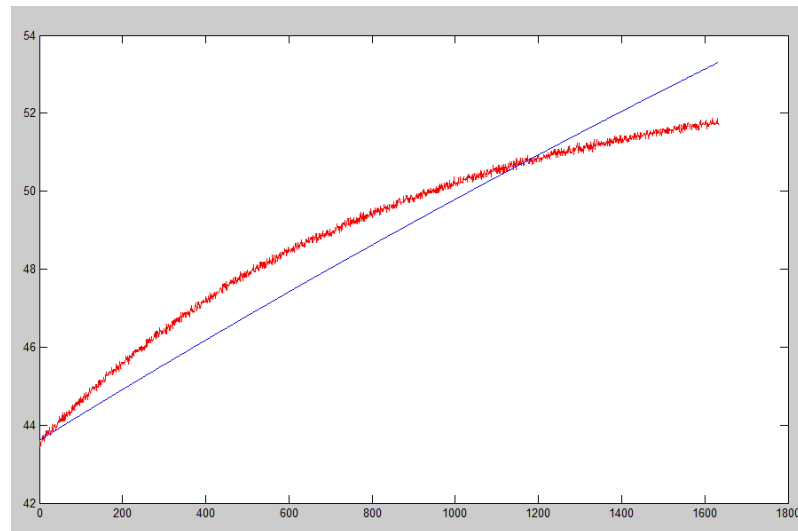


Figure 29: Result with the optimization method.

Another way of finding U and U' was to use the System Identification Tool. With a constant signal input u , this tool is able to provide the parameters K and p of the following expression:

$$y(t) = y(t_0) \cdot e^{pt} + K \cdot (u) \frac{e^{pt} - 1}{p} \quad (1.25)$$

where the constant signal input is $u = (T_1 + T_a)$ and the output is $(t) = T_f(t)$, in our case.

Though the parameter K doesn't match with the model described by the equation (1.24) (because K_1 and K_a are not the same), we may consider that the value of p provided by the tool is correct. In this case, we should be able to find K_1 and K_a , considering that :

$$p = f_1(U, U') \Rightarrow \exists f_2 : U' = f_2(U)$$

And considering f_2 ,

$$\left. \begin{array}{l} K_1 = f_3(U, U') \Rightarrow \exists f_4 : U = f_4(K_1) \\ K_a = f_5(U, U') \end{array} \right\} \Rightarrow \exists f_6 : K_a = f_6(K_1)$$

Then, injecting this expression of K_a in (1.24), the only unknown is K_1 and it can be found by using the System Identification Tool of MatLab.

This algorithm has been computed in a MatLab script called "*G_identification*" and is presented with the Annex 1.

Algorithm explanation:

First of all, the value of p , according to the expression (1.25), is found using the System Identification Tool.

The function f_1 is given by (1.18) and the function f_2 can be calculated for the given value of p . Since the expression of f_1 is quite complex, f_2 can't be easily deduced analytically. So, the method used was to find the values of U' which return the given

value of p in f_1 , for several values of U . In this way, we obtain several pairs of (U, U') which satisfy (1.18) and a polynomial approximation can be applied to these values to find f_2 , using the MatLab function *polyfit*.

The function f_3 is given by (1.17) and the function f_4 is found by calculating K_1 for different values of U , using f_2 , and by applying *polyfit* again to these values in order to find the polynomial approximation of f_4 .

The function f_5 is given by (1.19) and the function f_6 is found by calculating U for different values of K_1 and by applying *polyfit* again to these values in order to find the polynomial approximation of f_6 . f_6 can be approximated with a polynomial of the 1st degree, let $f_6 \equiv K_a = a_1 \cdot K_1 + a_0$.

Replacing f_6 in (1.24), we have

$$T_f(t) = T_{f_0} + (K_1 \cdot T_1 + (a_1 \cdot K_1 + a_0) \cdot T_a) \frac{e^{pt} - 1}{p}$$

$$T_f(t) - a_0 \cdot T_a \cdot \frac{e^{pt} - 1}{p} = T_{f_0} + K_1 \cdot (T_1 + a_1 \cdot T_a) \frac{e^{pt} - 1}{p}$$

which matches with the expression (1.25) with a constant input $u = (T_1 + a_1 \cdot T_a)$ and an output $y(t) = T_f(t) - a_0 \cdot T_a \cdot \frac{e^{pt} - 1}{p}$

Thus, this time, K_1 and p can be identified with the System Identification Tool. K_a , U and U' are then identified with f_6 , f_4 and f_2 , respectively.

The new value of p found by the System Identification Tool doesn't differ much from the previous one. Indeed, if we iterate 10 times the algorithm, the standard deviation of p is only 0.0022%.

Here are the final results provided by the algorithm:

$$p = -0.00119$$

$$K_1 = 0.00119$$

$$K_a = 7.77028e - 007$$

$$U = 133.37976 \text{ W/m}^2/\text{K}$$

$$U' = 88.58862 \text{ W/m}^2/\text{K}$$

The following figure shows that, with these parameters, the calculated values of T_f with (1.24) match the experiment:

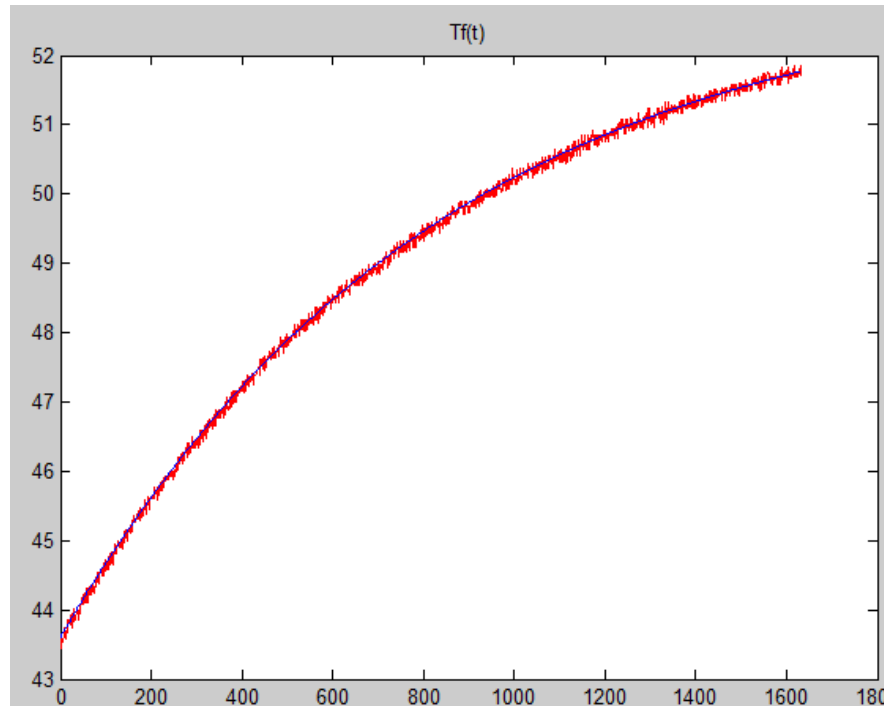


Figure 30: Result of the parameters identification of \mathbf{G} . (measured value of T_f in red and calculated value in blue)

5.4. The Boiler Model

5.4.1. *Modeling the Boiler*

The boiler already includes a PID controller to regulate the temperature of the water in the boiler. Let's consider the following scheme to analyze the boiler.

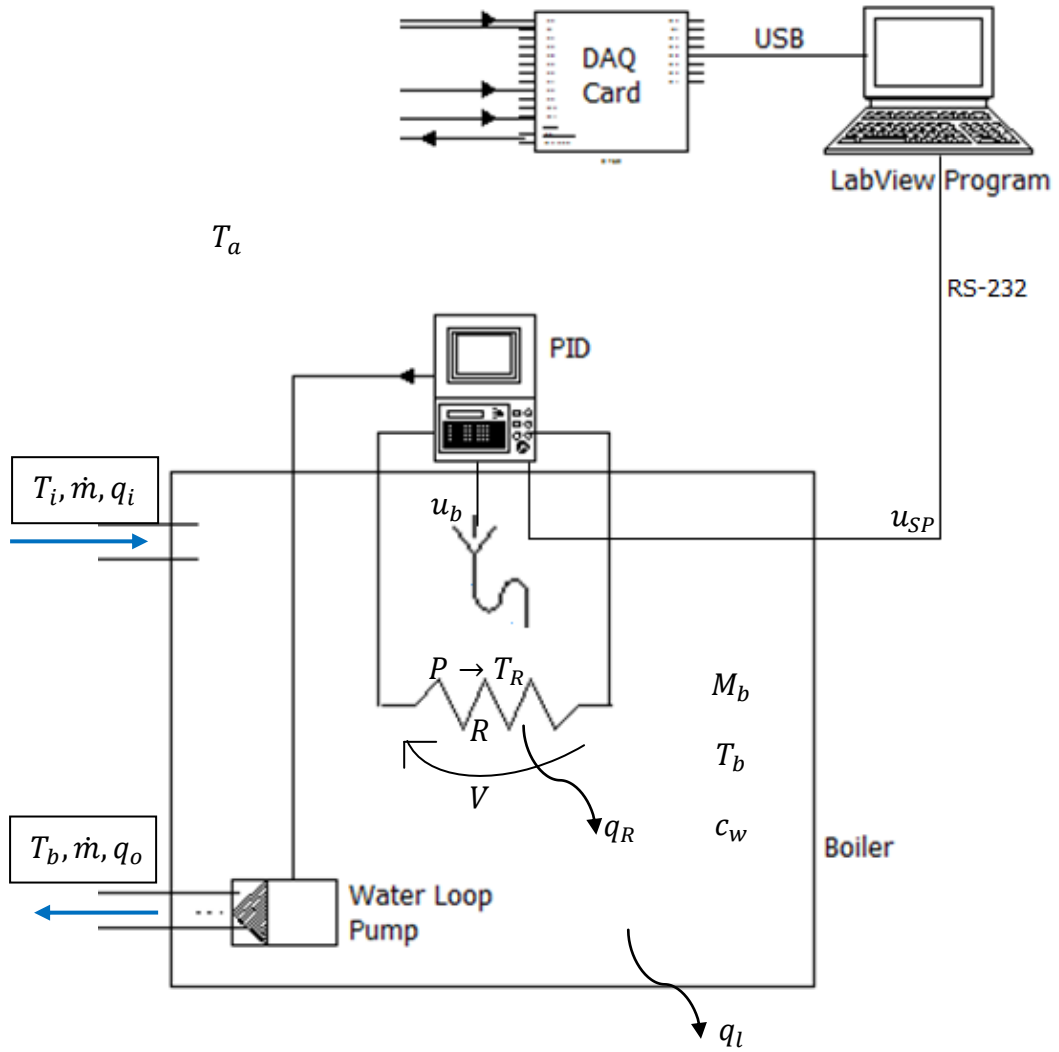


Figure 31: The functioning of the boiler

Let ...

$M_b[\text{kg}]$: The mass of water in the boiler.

$T_i, T_b [\text{K}]$: The temperatures at the input and in the boiler, respectively.

$q_i, q_o[\text{W}]$: The input and output rate of heat flow.

$q_l[\text{W}]$: The rate of heat flow lost due to the ambient air

$q_R[\text{W}]$: The rate of heat flow exchanged between the heating resistance and the water of the boiler

$R[\Omega]$: The value of the heating resistance

At the PID level, the temperature of the boiler T_b is controlled by two input signals: $u_{SP}[V]$ and $u_b[V]$, where u_b is the tension provided by the temperature sensor and u_{SP} is the tension provided by the LabView program and representing the setpoint temperature required by the LabView program for the controller. The control operation is based on the difference between these signals: $\varepsilon[V] = u_{SP} - u_b$. This difference is then amplified, integrated and derived adequately in order to generate the proper tension $V[V]$ used to reach the temperature setpoint effectively.

The tension V , through the resistance R , engenders a power $P[W] = \frac{V^2}{R}$. This power increases the temperature of the resistance T_R , allowing the water temperature to rise trough thermal exchange. The cooling operation is assured by the losses to the ambient air.

A quick analysis of the boiler let guess the following control scheme:

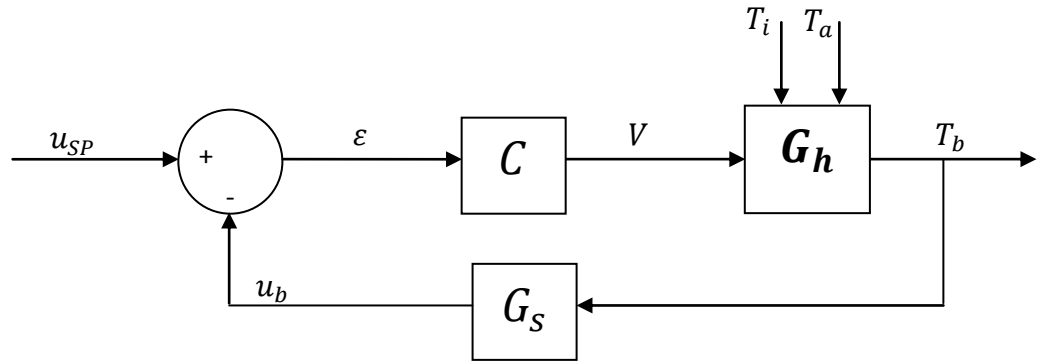


Figure 32: The supposed general control scheme of the boiler

Where C , G_h and G_s are the transfer functions of the PID controller, of the heater and of the temperature sensor, respectively.

The analytical expressions of C and G_s can be found quite easily:

- $C(s) = C_p \cdot \left(1 + \frac{1}{T_n \cdot s} + \frac{T_v \cdot s}{\tau_v \cdot s + 1} \right)$, which is the standard transfer function of a PID controller¹²

¹² (GOODWIN, et al., 2001)

- $G_s = \frac{K_s}{z.s+1}$, which is the standard transfer function of a temperature sensor.

However, since the transient response of the sensor is very fast compared to the response of the whole system, we can say $G_s \approx K_s$, which is the expression we will use in the following stages of the project.

The analytical expression of G_h is harder to find: we need to consider the mathematical relation ruling the temperature in the boiler. This can be found using the energy conservation law and the specific heat capacity definition:

$$\frac{c_w \cdot M_b \cdot dT_b}{dt} = q_i - q_o + q_R - q_l \quad (1.26)$$

And using the fundamental relation of heat exchangers¹³, we have

$$\frac{c_w \cdot M_b \cdot dT_b}{dt} = c_w \cdot \dot{m} \cdot (T_i - T_b) + U_R(T_R - T_b) \cdot A_R - U_b(T_b - T_a) \cdot A_b$$

where U_b [W/K/m²] and A_b [m²] are the exchange coefficient and the surface leading the temperature exchange with the ambient air and where U_r [W/K/m²] and A_r [m²] are the exchange coefficient and the surface leading the temperature exchange with the heating resistance.

We need to know $T_b = f(V, T_i, T_a)$. So, let's try to express T_R in terms of V ...

T_R should be the result of the integration of the power generated and of the rate of heat flow occurring with the water :

$$c_w \cdot \dot{m} \cdot dT_R = P \cdot dt - q_R \cdot dt$$

$$T_R = \int_0^{T_R} dT_R = \frac{1}{c_w \cdot \dot{m}} \cdot \left(\int_0^t \frac{V^2}{R} \cdot dt - \int_0^t q_R \cdot dt \right)$$

However, we see that this relation of V to T_R will engender a non-linear model. Moreover, the presence of the integral prevents us linearizing the model around an operating point without significant errors. The model is too complex.

¹³ (KELNER, 2011)

We can simplify the model by considering that the power P is directly used to heat the water up. In this case, we have $P = q_R$.

The equation (1.26) then becomes,

$$\frac{c_w \cdot M_b \cdot dT_b}{dt} = c_w \cdot \dot{m} \cdot (T_i - T_b) + \frac{V^2}{R} - U_b(T_b - T_a) \cdot A_b \quad (1.27)$$

5.4.2. Determining the heater transfer function

Let's try to break down the heater scheme as follow:

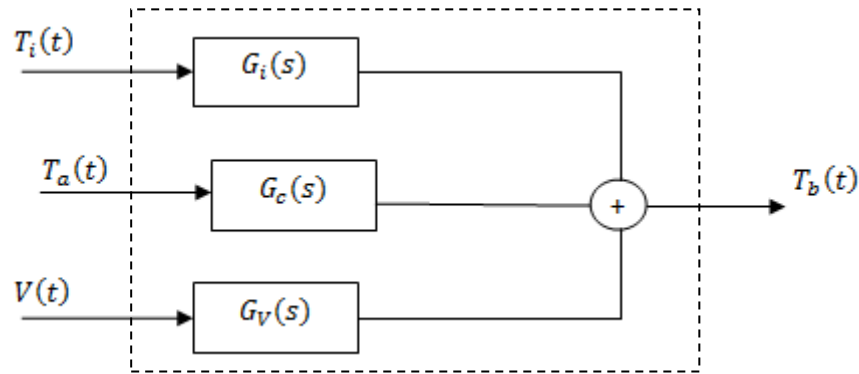


Figure 33: The supposed control scheme of the heater, with separate signals

To find the transfer function to each input V, T_i and T_a , we can apply the Laplace transform on the previous expression...

$$c_w \cdot M_b \cdot (s \cdot \mathcal{T}_b - T_{b_0}) = c_w \cdot \dot{m} \cdot (\mathcal{T}_i - \mathcal{T}_b) + \frac{\mathcal{L}[V^2]}{R} - U_b(\mathcal{T}_b - \mathcal{T}_a) \cdot A_b$$

...and cancel, each time, the others inputs. This way, we find, considering zero initial conditions:

$$G_i = \frac{\mathcal{T}_b}{\mathcal{T}_i} = \frac{c_w \cdot \dot{m}}{c_w \cdot M_b \cdot s + c_w \cdot \dot{m} + U_b \cdot A_b} = \frac{K_i}{s - p_i}$$

$$G_c = \frac{\mathcal{T}_b}{\mathcal{T}_a} = \frac{U_b \cdot A_b}{c_w \cdot M_b \cdot s + c_w \cdot \dot{m} + U_b \cdot A_b} = \frac{K_c}{s - p_c}$$

Where

$$\boxed{K_i = \frac{\dot{m}}{M_b} ; K_c = \frac{U_b \cdot A_b}{c_w \cdot M_b} ; p_i = p_c = (p') = -\frac{c_w \cdot \dot{m} + U_b \cdot A_b}{c_w \cdot M_b}}$$

Concerning the transfer function to the input V , the model doesn't provide a linear relation :

$$c_w \cdot M_b \cdot s \cdot \mathcal{T}_b = -c_w \cdot \dot{m} \cdot (\mathcal{T}_b) + \frac{\mathcal{L}[V^2]}{R} - U_b(\mathcal{T}_b) \cdot A_b \quad (1.28)$$

Hence, we should linearize the relation around an operating point in order to get an simple enough model for control purposes.

However, further analysis of the boiler revealed that the output of the controller isn't the voltage V but the power P at the heating resistance. Indeed, if we observe for example the proportional action of the PID controller, we can see that it is the heating power P which is proportional to the PID input ε , and not to the voltage V .

This important modification of the model leads to the following schemes:

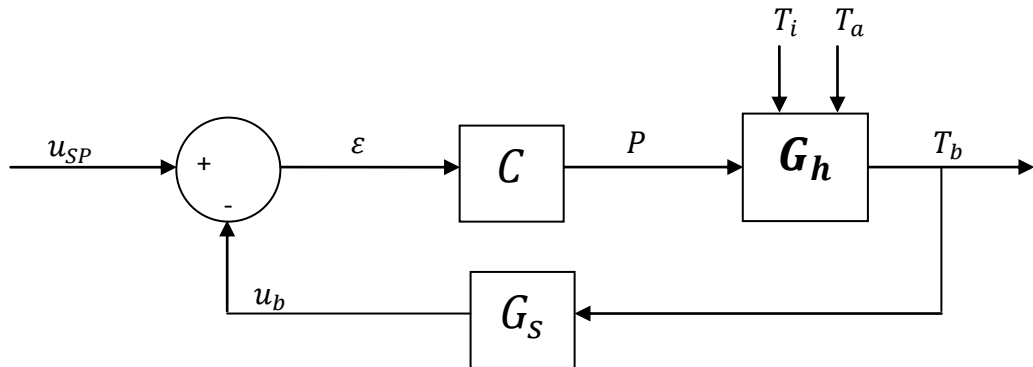


Figure 34: The real general control scheme of the boiler

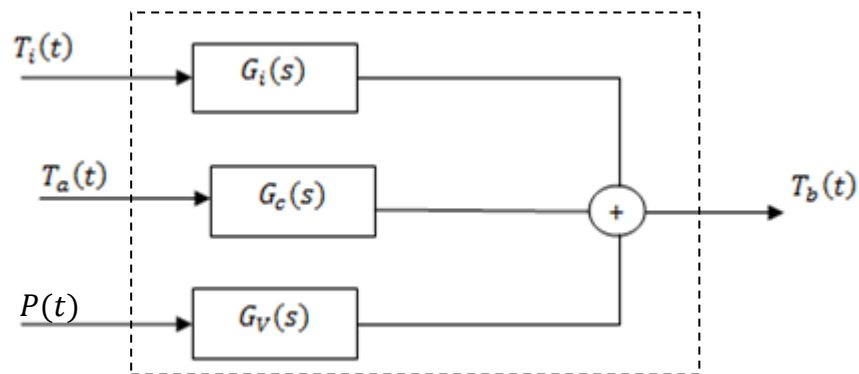


Figure 35: The real control scheme of the heater, with separate signals¹⁴

¹⁴ Non-small-signal model

where G_i and G_c have the same expression as determined above.

And for the transfer function G_V to the third input $P(t)$, the expression of (1.27),

$$\frac{c_w \cdot M_b \cdot dT_b}{dt} = c_w \cdot \dot{m} \cdot (T_i - T_b) + P - U_b(T_b - T_a) \cdot A_b$$

leads, this time, to a linear model where G_V is easy to determine:

$$c_w \cdot M_b \cdot s \cdot \mathcal{T}_b = -c_w \cdot \dot{m} \cdot (\mathcal{T}_b) + \mathcal{P} - U_b(\mathcal{T}_b) \cdot A_b$$

$$G_V = \frac{\mathcal{T}_b}{\mathcal{P}} = \frac{1}{c_w \cdot M_b \cdot s + c_w \cdot \dot{m} + U_b \cdot A_b} = \frac{1}{s - p'}$$

This behavior of the PID controller was discovered quite late in the project and a lot of work was done to linearize the non-linear model, to understand and integrate the consequences of a small-signal model and to define a proper operating point Q for the purpose of linearization.

That's why the work accomplished in this field is shown in "Annex 2 : Example of a Non-linear Model". Even if this part of work may seem useless for this project, it permitted the student to approach the non-linear models and their implications, to experiment a linearization method, to deal with the small-signal model concept and to understand how to choose a proper operating point the purpose of linearization. These are all the reasons why the work accomplished in this field is highlighted in annex.

5.4.3. *Determining the parameters for the boiler*

Direct parameters :

Concerning the heater transfer function, it depends on the parameters $c_w, \dot{m}, M_b, A_b, U_b$.

c_w and \dot{m} have already been determined in 5.2.2.

$$M_b = 10,5 \text{ l}$$

$$A_b = 0,542 \text{ m}^2$$

U_b is a little bit harder to find and is the object of the following paragraph.

Parameters of G_c :

Both parameters K_c and p_c have to be determined, where U_b is the only unknown. In order to achieve this goal, a test called “*Air test*” has been performed (available in Annex 1). In this test, neither the heater nor the pump are used ($P = 0$ and $\dot{m} = 0$). The boiler, filled with hot water is just cooled down by the ambient air.

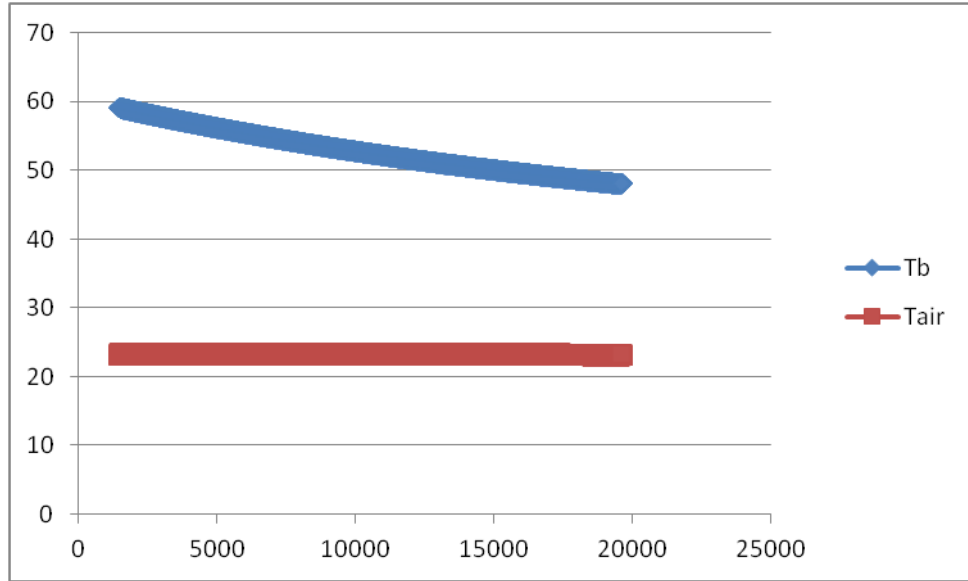


Figure 36: Cooling behavior of the boiler (alone)

So the equation (1.27) ruling the temperature in the boiler becomes:

$$\frac{c_w \cdot M_b \cdot dT_b}{dt} = - U_b (T_b - T_a) \cdot A_b$$

Applying the Laplace Transform:

$$c_w \cdot M_b \cdot (s \cdot \mathcal{T}_b - T_{b_0}) = - U_b (\mathcal{T}_b - \mathcal{T}_a) \cdot A_b$$

Considering that $K_c = \frac{U_b \cdot A_b}{c_w \cdot M_b}$:

$$\mathcal{T}_b = \frac{K_c}{s + K_c} \cdot \mathcal{T}_a + \frac{T_{b_0}}{s + K_c}$$

The test revealed that T_a can be considered as constant:

$$\mathcal{T}_b = \frac{K_c}{s + K_c} \cdot \frac{T_a}{s} + \frac{T_{b_0}}{s + K_c}$$

Applying partial fraction decomposition :

$$\mathcal{T}_b = \frac{-T_a}{s + K_c} + \frac{T_a}{s} + \frac{T_{b_0}}{s + K_c}$$

And applying the inverse Laplace Transform, we find the equation of $T_b(t)$:

$$T_b(t) = T_{b_0} \cdot e^{-K_c t} - T_a \cdot (e^{-K_c t} - 1)$$

This equation can be used in the System Identification Tool of Matlab to find K_c , using the input T_a and the output T_b . The value of K_c provided by the tool (2.0498e-005) leads to a good co-relation between the measurements and the calculation:

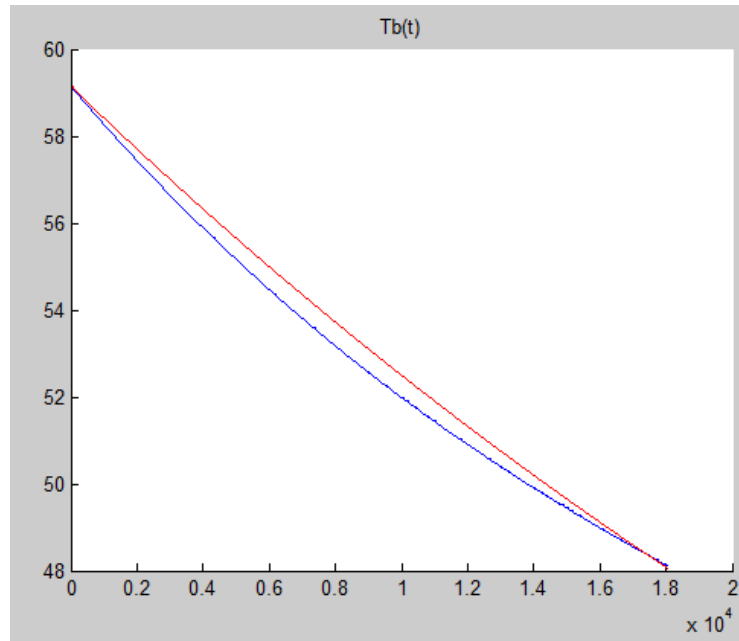


Figure 37: Air test results. Measured values of T_b in blue and calculated values in red

From K_c , we can now deduce the values of U_b and p_c :

$$K_c = \frac{U_b \cdot A_b}{c_w \cdot M_b} = 2.04984 \cdot 10^{-5} \Rightarrow U_b = 1.66071 \text{ W/m}^2/\text{K}$$

$$p_c = -\frac{c_w \cdot \dot{m} + U_b \cdot A_b}{c_w \cdot M_b} = -0.001965$$

Parameters of G_i :

$$K_i = \frac{\dot{m}}{M_b} = 0,00194$$

$$p_i = p_c = -0.00197 = p'$$

Parameters of G_v :

$$p' = -0.001965$$

Parameter of G_s :

The gain of G_s , K_s , depends directly on the scale used to represent the temperature T_b by a tension u_b . However, this sensor can't be technically acceded because it is part of the boiler. That's why we will symbolize the values of u_b by the temperature values to which they refer. For example, the tension generated by the sensor due to a boiler temperature of 53°C will be noted $u_b = (53^\circ C)_{[V]}$. The subscript $[V]$ is used to remember that the value refers to a tension in volts. Misuse of terms, could lead to writing $u_b = 53$ too. The same convention is used for the tension u_{SP} , since u_{SP} can't be measured either because of the serial communication.

With this convention, it follows that $K_s = 1$.

Parameter of C :

$$C(s) = C_p \cdot \left(1 + \frac{1}{T_n \cdot s} + \frac{T_v \cdot s}{\tau_v \cdot s + 1} \right)$$

The parameters of the controller can be adjusted using the key pad of the boiler. For this project, we kept the default configuration, i.e. :

$$T_n = 100s$$

$$T_v = 10s$$

The constructor indicated that the relation between τ_v and T_v : $\tau_v = 0,2T_v = 2s$

For the proportional component, it is the *proportional band PB* which is entered.
*"The proportional band PB[%] is defined as the error required (as a percentage of full scale) to yield a 100% change in the controller output"*¹⁵

From the proportional range, we can deduce the value of C_p , with the formula provided by the reference book :

$$PB[\%] = \frac{PB}{FS} = \frac{100[\%]}{C_p} \Rightarrow C_p = \frac{100.FS}{PB}$$

where FS is the full scale.

The default value of PB is $PB = 1$. And the full range is $FS = 40$ (determined by tests, by cancelling out the integrative and derivative components). So,

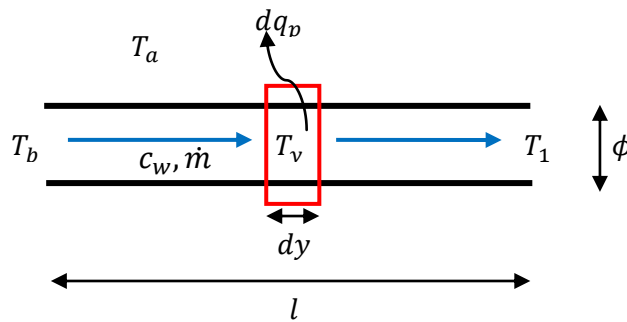
$$C_p = 4000$$

5.5. The Pipes Model

5.5.1. *Modeling the pipes*

Between the boiler and the fermentor, the water is prone to cooling from T_b to T_1 , in the water loop pipe. This cooling depends on the ambient temperature T_a .

Let's consider an infinitesimal length dy of the pipe :



Let :

dy [m]: The length of the infinitesimal length of the pipe.

T_y [K]: The temperature of the infinitesimal length

¹⁵ (GOODWIN, et al., 2001)

dq_p [W] : The heat lost by the infinitesimal height due to of the ambient air

l [m]: The length of the pipe.

ϕ [m]: The diameter of the pipe.

The specific heat capacity definition gives:

$$dq_p = -c_w \cdot \dot{m} \cdot dT_y \quad (1.29)$$

where dT_y is the temperature difference between two neighboring infinitesimal lengths.

The fundamental relation of the heat exchangers¹⁶ gives :

$$dq_p = U_p \cdot (T_y - T_a) \cdot \phi \cdot \pi \cdot dy \quad (1.30)$$

where U_p [W/m²K] is the exchange coefficient leading the heat exchange between the pipe and the ambient air.

Assembling (1.29) and (1.30) and integrating on the whole length of the pipe gives:

$$\int_{T_b}^{T_1} \frac{dT_y}{T_y - T_a} = \frac{-U_p \cdot \phi \cdot \pi}{c_w \cdot \dot{m}} \cdot \int_0^l dy$$

If we consider U_p constant all along the pipe:

$$\frac{T_1 - T_a}{T_b - T_a} = e^{\frac{-U_p \cdot \phi \cdot \pi \cdot l}{c_w \cdot \dot{m}}} \quad (1.31)$$

$$T_1 = T_a \cdot \left(1 - e^{\frac{-U_p \cdot \phi \cdot \pi \cdot l}{c_w \cdot \dot{m}}} \right) + T_b \cdot e^{\frac{-U_p \cdot \phi \cdot \pi \cdot l}{c_w \cdot \dot{m}}}$$

¹⁶ (KELNER, 2011)

5.5.2. Identification of the transfer function of the pipe

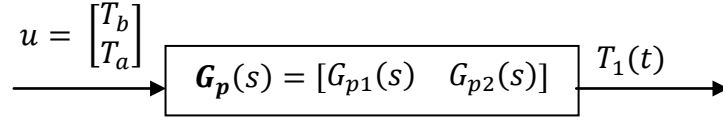


Figure 38: Control scheme of the pipe, matrix point of view.

Once again, we need to apply the Laplace Transform, after cancelling out first input, then the other:

$$G_{p1}(s) = \frac{\mathcal{T}_1}{\mathcal{T}_b} = e^{\frac{-U_p \cdot \phi \cdot \pi \cdot l}{c_w \cdot \dot{m}}} = K_{p1}$$

$$G_{p2}(s) = \frac{\mathcal{T}_1}{\mathcal{T}_a} = 1 - e^{\frac{-U_p \cdot \phi \cdot \pi \cdot l}{c_w \cdot \dot{m}}} = K_{p2}$$

5.5.3. Determining the parameters of the pipe

The parameters involved are c_w, \dot{m}, U_p, ϕ and l .

c_w and \dot{m} have already been determined in 5.2.2.

$$\phi = 0,01m$$

$$l = 4m$$

Concerning U_p , we know that $T_a = 23^\circ C$ and $T_b = 53^\circ C$ involve $T_1 = 51,2^\circ C$. So, from (1.31), we have :

$$U_p = \frac{-c_w \cdot \dot{m}}{\phi \cdot \pi \cdot l} \ln \left(\frac{T_1 - T_a}{T_b - T_a} \right) = 42.0429 \text{ W/m}^2/\text{K}$$

And

$$K_{p1} = 0.94$$

$$K_{p2} = 0.06$$

5.6. Modeling the transfer function of T_2

The operation of the boiler depends on its input T_i . The temperature T_i is not independent of the system: it is the result of T_2 subject to the ambient air in the back pipe, that is G_p since the two pipes are identical:

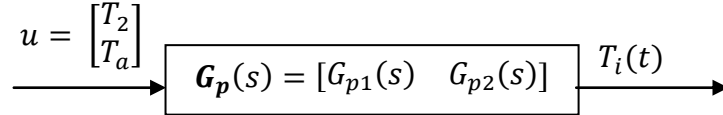


Figure 39: Control scheme of the back pipe, matrix point of view.

As for T_2 , it depends on three variables, as the equation (1.14) shows :

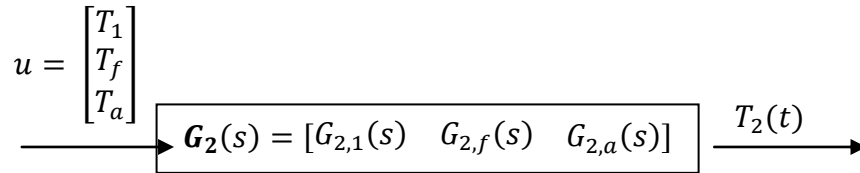


Figure 40: Control scheme giving T_2 , matrix point of view.

$G_2(s)$ is directly given by (1.14), after applying the Laplace Transform and cancelling out each input one after the other :

$$G_{2,1}(s) = \frac{\mathcal{T}_2}{\mathcal{T}_1} = e^{hb} = K_{2,1}$$

$$G_{2,f}(s) = \frac{\mathcal{T}_2}{\mathcal{T}_f} = \left(\frac{(U.R)}{(U.R + U'.R')} - \frac{(U.R)}{(U.R + U'.R')} e^{hb} \right) = K_{2,f}$$

$$G_{2,a}(s) = \frac{\mathcal{T}_2}{\mathcal{T}_a} = \left(\frac{(U'.R')}{(U.R + U'.R')} - \frac{(U'.R')}{(U.R + U'.R')} \cdot e^{hb} \right) = K_{2,a}$$

where all the parameters are already determined :

$$K_{2,1} = 0.64140$$

$$K_{2,f} = 0.18331$$

$$K_{2,a} = 0.17529$$

5.7. Conclusion

Assembling the models leads to the following model:

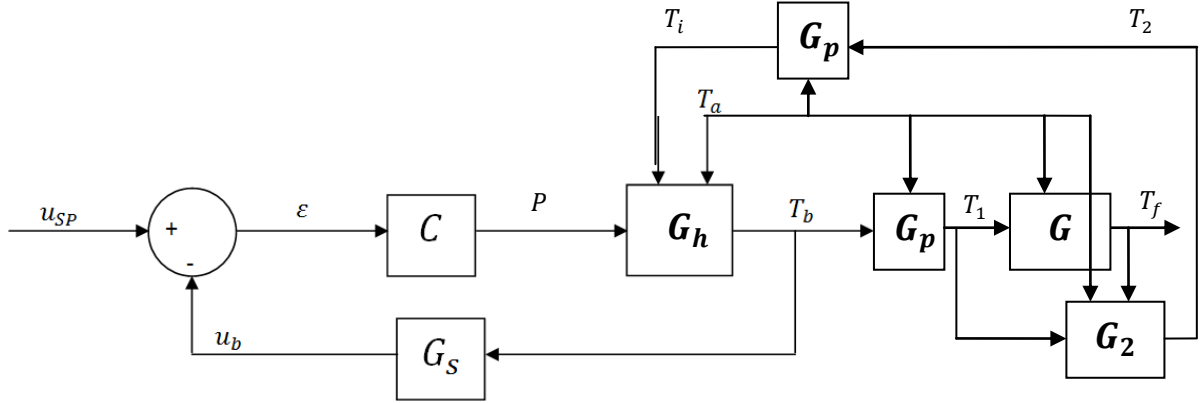


Figure 41: Global control scheme of the system

Let's remember all the values of these transfer functions :

$$C(s) = 4000. \left(1 + \frac{1}{100.s} + \frac{10.s}{2.s + 1} \right)$$

$$G_s(s) = K_s = 1$$

G_h , G_p , G and G_2 are matrices. If we consider, respectively, the inputs vector

$$\begin{bmatrix} P \\ T_i \\ T_a \end{bmatrix}, \begin{bmatrix} T_b \text{ or } T_2 \\ T_a \end{bmatrix}, \begin{bmatrix} T_1 \\ T_a \end{bmatrix} \text{ and } \begin{bmatrix} T_1 \\ T_f \\ T_a \end{bmatrix} :$$

$$\begin{aligned} G_h(s) &= [G_v \quad G_i \quad G_c] = \begin{bmatrix} \frac{1}{s-p'} & \frac{K_i}{s-p'} & \frac{K_c}{s-p'} \end{bmatrix} \\ &= \begin{bmatrix} \frac{1}{s + 0.0019650} & \frac{0.0019445}{s + 0.0019650} & \frac{2.0498e-5}{s + 0.0019650} \end{bmatrix} \end{aligned}$$

$$G_p(s) = [K_{p1} \quad K_{p2}] = [0.94 \quad 0.06]$$

$$G(s) = [G_1 \quad G_a] = \begin{bmatrix} \frac{K_1}{s-p} & \frac{K_a}{s-p} \end{bmatrix} = \begin{bmatrix} \frac{0.0011943}{s + 0.0011918} & \frac{7.7703e-7}{s + 0.0011918} \end{bmatrix}$$

$$G_2(s) = [K_{2,1} \quad K_{2,f} \quad K_{2,a}] = [0.64140 \quad 0.18331 \quad 0.17529]$$

This global control scheme has been introduced in Simulink for the purpose of analysing (available in Annex 1). In order for this Simulink model to fit with the real plant, saturation conditions have to be imposed to the PID controller. Indeed, range of the power P can only be between 0W and 2000W. The PID controller saturates under and beyond these both limits respectively.

6. Control Design

6.1. Global scheme simplification

The purpose of this paragraph is to simplify the global control scheme of the Figure 41 as follows:

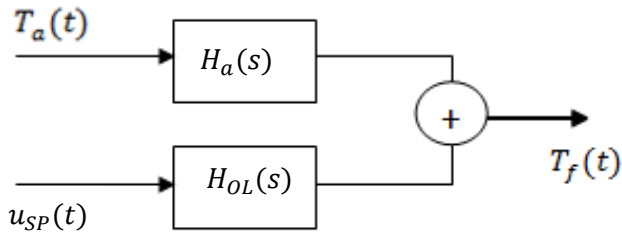


Figure 42: Simplified global control scheme of the system

From the global scheme, if we cancel out the input T_a , we have the following equations:

$$\mathcal{T}_f = \mathcal{T}_b \cdot K_{p1} \cdot G_1 \quad (1.32)$$

$$\mathcal{T}_b = \mathcal{T}_i + (u_{SP} - \mathcal{T}_b) \cdot C \cdot G_V \quad (1.33)$$

$$\mathcal{T}_i = (\mathcal{T}_b \cdot K_{p1} \cdot K_{2,1} + \mathcal{T}_f \cdot K_{2,f}) \cdot K_{p1} \cdot G_i \quad (1.34)$$

Thus, from (1.32) and (1.34):

$$\mathcal{T}_i = (\mathcal{T}_b \cdot K_{p1} \cdot K_{2,1} + \mathcal{T}_b \cdot K_{p1} \cdot G_1 \cdot K_{2,f}) \cdot K_{p1} \cdot G_i$$

And with (1.33) :

$$\frac{\mathcal{T}_b}{u_{SP}} = \frac{C \cdot G_V}{1 - K_{p1} \cdot K_{2,1} K_{p1} \cdot G_i - K_{p1} \cdot G_1 \cdot K_{2,f} K_{p1} \cdot G_i + C \cdot G_V}$$

Finally, with (1.32)

$$H_{OL}(s) = \frac{\mathcal{T}_f}{u_{SP}} = \frac{C \cdot G_V \cdot K_{p1} \cdot G_1}{1 - K_{p1} \cdot K_{2,1} K_{p1} \cdot G_i - K_{p1} \cdot G_1 \cdot K_{2,f} K_{p1} \cdot G_i + C \cdot G_V}$$

Calculating with MatLab, we have:

$$H_{OL}(s) = \frac{26.9435}{(s + 24000) \cdot (s + 0.001192)}$$

which is a transfer function with two poles of very different orders of size. It can therefore be simplified to a first order transfer function...

$$H_{OL}(s) = \frac{\frac{26.9435}{24000}}{\left(\frac{s}{24000} + 1\right) \cdot (s + 0.001192)}$$

since $\left(\frac{s}{24000} + 1\right) \approx 1$:

$$H_{OL}(s) = \frac{0.001123}{(s + 0.001192)}$$

Also, if we cancel out the input u_{SP} , we have the following equations :

$$\mathcal{T}_b = G_i \cdot \mathcal{T}_i + G_c \cdot \mathcal{T}_a - C \cdot G_V \cdot \mathcal{T}_b \quad (1.35)$$

$$\mathcal{T}_i = K_{p2} \cdot \mathcal{T}_a + K_{p1} \cdot \mathcal{T}_2 \quad (1.36)$$

$$\mathcal{T}_2 = K_{2,a} \cdot \mathcal{T}_a + K_{2,1} \cdot \mathcal{T}_1 + K_{2,f} \cdot \mathcal{T}_f \quad (1.37)$$

$$\mathcal{T}_f = G_1 \cdot \mathcal{T}_1 + G_a \cdot \mathcal{T}_a \quad (1.38)$$

$$\mathcal{T}_1 = K_{p2} \cdot \mathcal{T}_a + K_{p1} \cdot \mathcal{T}_b \quad (1.39)$$

From (1.38) and (1.39),

$$\mathcal{T}_f = G_1 \cdot (K_{p2} \cdot \mathcal{T}_a + K_{p1} \cdot \mathcal{T}_b) + G_a \cdot \mathcal{T}_a$$

$$\mathcal{T}_b = \frac{\frac{\mathcal{T}_f - G_a \cdot \mathcal{T}_a}{G_1} - K_{p2} \cdot \mathcal{T}_a}{K_{p1}} \quad (1.40)$$

From (1.35), (1.36), (1.37) and (1.39):

$$\mathcal{T}_b = \frac{G_i \left(K_{p2} \cdot \mathcal{T}_a + K_{p1} (K_{2,a} \cdot \mathcal{T}_a + K_{2,1} (K_{p2} \cdot \mathcal{T}_a) + K_{2,f} \cdot \mathcal{T}_f) \right) + G_c \cdot \mathcal{T}_a}{1 + C \cdot G_V - K_{p1} K_{2,1} K_{p1} G_i}$$

And with (1.40),

$$\frac{\frac{\mathcal{T}_f - G_a \cdot \mathcal{T}_a}{G_1} - K_{p2} \cdot \mathcal{T}_a}{K_{p1}} = \frac{G_i \left(K_{p2} \cdot \mathcal{T}_a + K_{p1} (K_{2,a} \cdot \mathcal{T}_a + K_{2,1} (K_{p2} \cdot \mathcal{T}_a) + K_{2,f} \cdot \mathcal{T}_f) \right) + G_c \cdot \mathcal{T}_a}{1 + C \cdot G_V - K_{p1} K_{2,1} K_{p1} G_i}$$

$$\mathcal{T}_f = G_a \cdot \mathcal{T}_a + G_1 \left(K_{p2} \cdot \mathcal{T}_a + K_{p1} \cdot \frac{G_i \left(K_{p2} \cdot \mathcal{T}_a + K_{p1} (K_{2,a} \cdot \mathcal{T}_a + K_{2,1} (K_{p2} \cdot \mathcal{T}_a) + K_{2,f} \cdot \mathcal{T}_f) \right) + G_c \cdot \mathcal{T}_a}{1 + C \cdot G_V - K_{p1} K_{2,1} K_{p1} G_i} \right)$$

$$H_a(s) = \frac{\mathcal{T}_f}{\mathcal{T}_a} = \frac{G_a + G_1 K_{p2} + \frac{G_1 K_{p1} G_i K_{p2} + G_1 K_{p1} G_i K_{p1} K_{2,a} + G_1 K_{p1} G_i K_{p1} K_{2,1} K_{p2} + G_1 K_{p1} G_c}{1 + C \cdot G_V - K_{p1} K_{2,1} K_{p1} G_i}}{1 - \frac{G_1 K_{p1} G_i K_{p1} K_{2,f}}{1 + C \cdot G_V - K_{p1} K_{2,1} K_{p1} G_i}}$$

which leads to an expression with 13 roots, with one of them entirely real and 14 poles, with two of them entirely real.

It is important to understand that these two transfer functions don't take into account the saturation of the PID controller explained in 5.7. Indeed, if we compare, for example, the step response of H_a with that provided by the Simulink model to a step input of T_a (u_{sp} cancelled), we can note the difference :

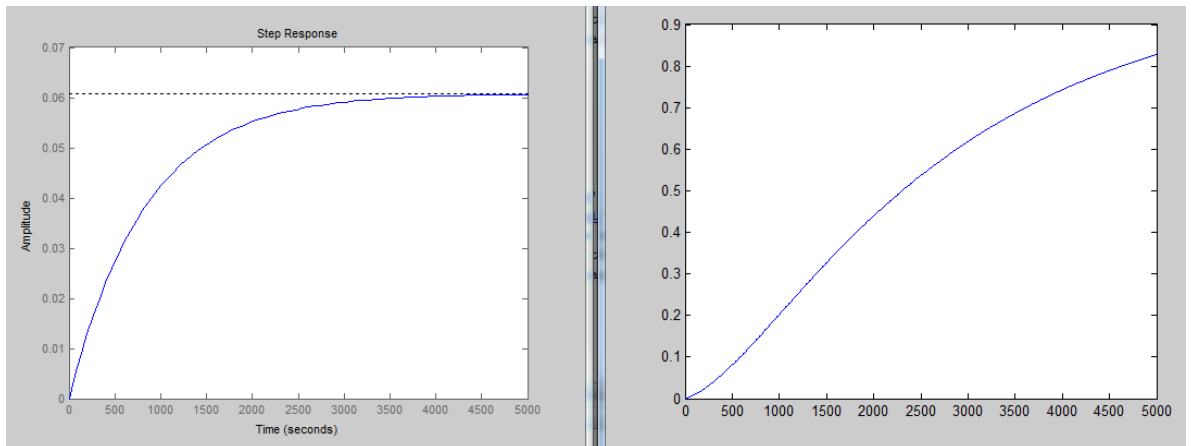


Figure 43 : Highlighting the saturation impact. Left: H_a step response ; Right : the corresponding response with the Simulink model.

We can still however verify that the calculation of H_a and H_{OL} are correct by comparing their step responses with that provided by the Simulink model but without using the saturation constraints.

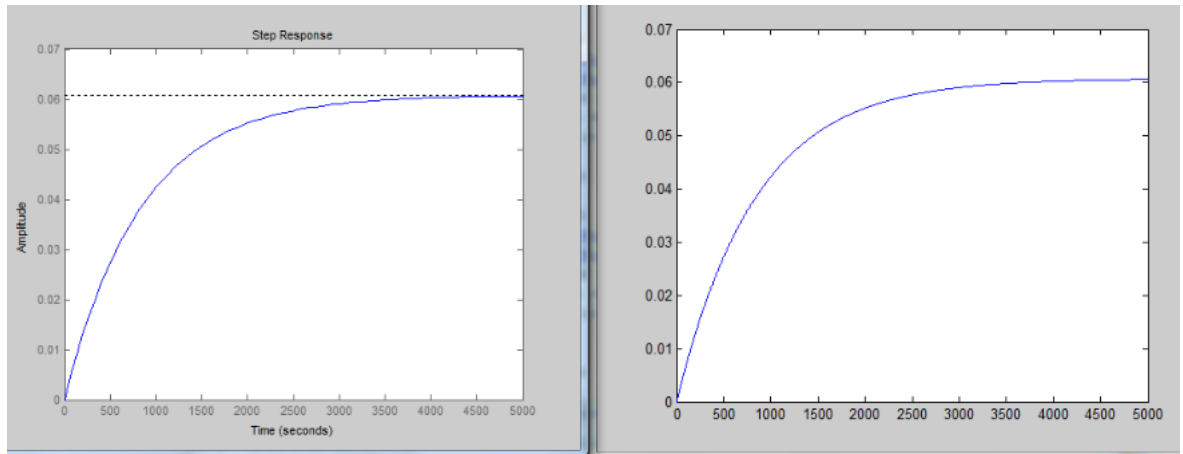


Figure 44 : H_a verification

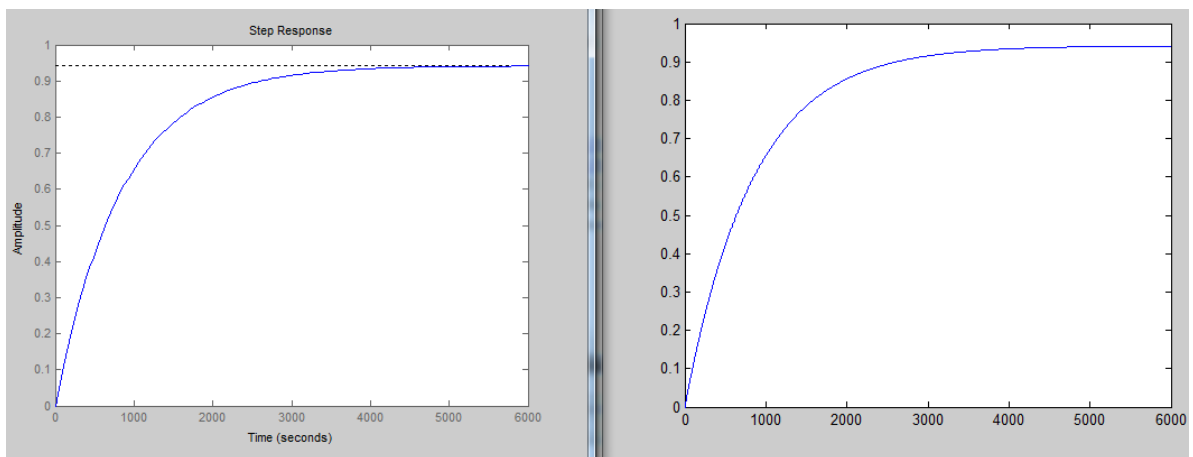


Figure 45 : H_{OL} verification

These comparisons only allow us to verify that the calculation of H_a and H_{OL} are correct. These two transfer functions can be used for analysis purposes only if the signal P stays in the range 0-2000W. That's why we will prefer to base our further analysis on the Simulink model instead of on the simplified transfer functions.

6.2. PID generalities

In the regulation and control industry, the PID (PI) controller has definitely imposed itself as the main means of regulation. Indeed, it has already proved its efficiency, simplicity and robustness for a large scope of systems in various fields.

"PID" stands for *Proportional-Integrative-Derivative*. Indeed, the regulation is based on the current error value, e , on the integral of these errors and on the derivative of the error at the same time. The error represents the difference between the set point

value (which the user wants) and the real output. That's why a PID controller uses to be applied in a feedback loop:

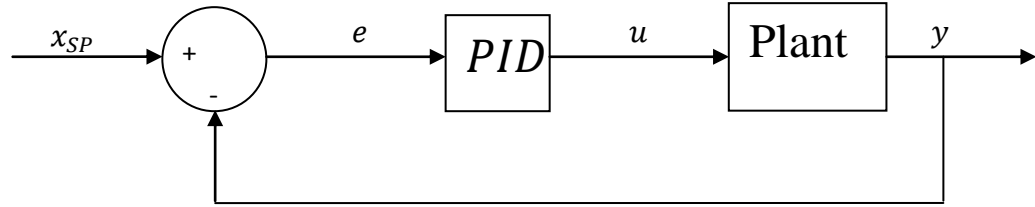


Figure 46: Use of a PID in a feedback loop

The scheme of a PID can be broken down as follows¹⁷ :

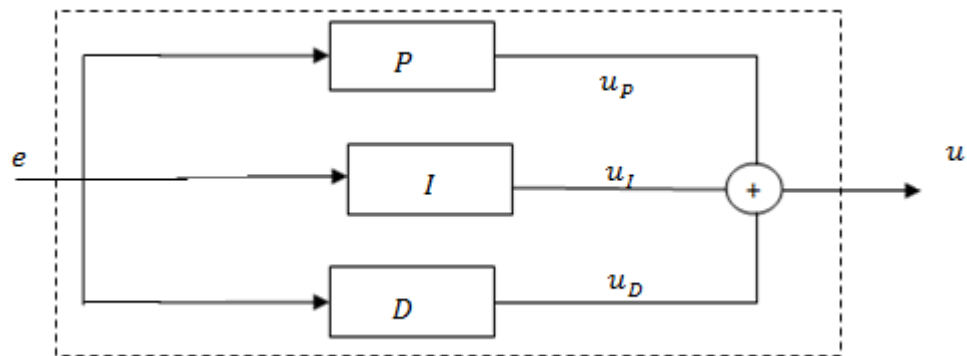


Figure 47: Detailed scheme of a PID.

where the effects of each component P, I and D can be explained by the three following three laws :

$$u_P(t) = K_P \cdot e(t)$$

$$u_I(t) = K_I \cdot \int_0^t e(t) dt$$

$$u_D(t) = K_D \cdot \frac{d}{dt} e(t)$$

K_P , K_I and K_D are the parameters of the PID controller. Their determinations are subject to the PID designing.

Let's remember the effects of each component P, I and D.

¹⁷ (VETCOUR, 2011-2012)

The proportional component provides an output which depends on the instantaneous value of the error. So, it allows fast correction of every error. A large value for K_p permits adjusting the correction faster but a too large value generates overshoots and instability. The proportional component alone provides a response which presents a nonzero steady-state error.

The integrative component provides an output which is proportional to the accumulated error. This means that the integrative component is a “slow mode” because the error needs enough time to be accumulated to provide a significant effect. However, for an infinite time, that is for the steady state, the integrative component allows cancelling the error out. Indeed, while an error persists, its output continues evolving till the error is cancelled out. The integrative component presents the drawbacks of decreasing the stability of the system and other undesirable effects, like the wind-up effect, which is specific to this component.

Finally, the derivative component allows anticipating the evolution of the output since this component reacts to the rate of change of the error. This predictive mode is also considered as a “fast mode” since it evolves quickly when the error evolves fast and it disappears when the error tends to be constant. This component allows increasing the stability of the system and limiting the overshoots, which are precisely the drawbacks of the two previous components. Since the action of the derivative is bonded to the rate of change of the error, it should not be used for the control of variables presenting too much noise or varying too fast (or by steps).

The three previous laws lead to the parallel transfer function of a PID controller :

$$PID(s) = K_p + \frac{K_I}{s} + K_D \cdot s$$

The design of the PID controller will consist of finding accurate values for the parameters K_p and K_I (and K_D).

6.3. Closed loop

For simplicity and time reasons, it has been chosen to use a PI controller and not to use the derivative component of a PID controller. This controller will be implemented thanks to LabView. Digital PI controllers are available in the LabView library. The digital approach in regulation is similar to the continuous-time approach in considering a short enough small sampling time compared to the system speed. In our case, we have chosen a sampling time of 1s for all the variables, which can be considered as sufficiently short, given the slowness of the system (temperature evolutions).

As explained in 3.2, the control strategy is to regulate the boiler setpoint temperature in order to keep as much as possible a constant temperature of 53°C inside the fermentor.

Using a PI controller for this purpose leads to the following closed loop scheme:

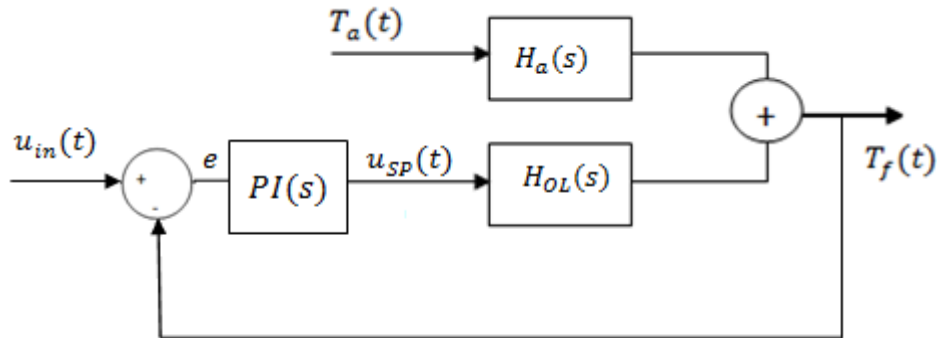


Figure 48: Intuitive closed-loop scheme

We see that the output of the PI controller is the setpoint value for the boiler temperature. Our new PI controller is connected in series with the existing boiler controller. We can see that this closed loop is not adequate for our regulation issue. Indeed, when we have $T_f = u_{in}$, the output of the PI controller is 0. This means that the controller asks the boiler to reach 0°C, which is not appropriate. In this case, the output of the PI controller should be the boiler temperature which leads to $T_f = u_{in}$ in the steady state, let T_{bQ} . Let's modify our closed loop scheme in consequence:

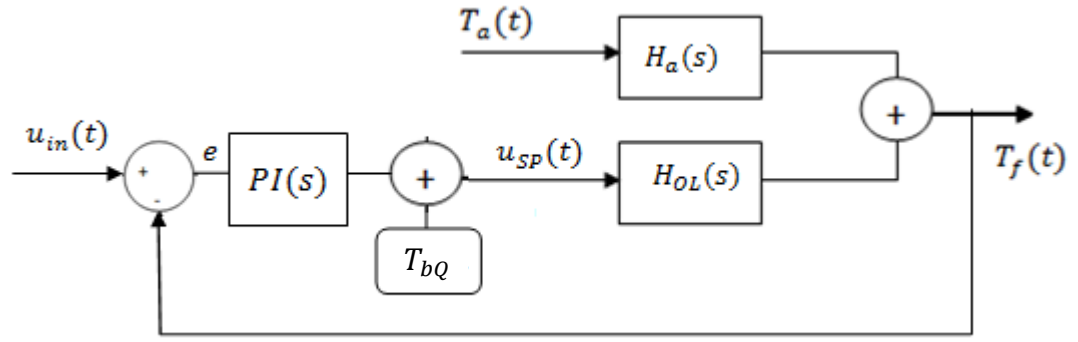


Figure 49 : Closed loop scheme

We know from the ATC configuration that the relation between T_1 and T_b is given by the equation (1.1), for the temperature $T_a = 23^\circ\text{C}$:

$$T_{bQ} = \frac{T_{1Q} - 1,38}{0,94}$$

where T_{1Q} is the value of T_1 in steady state; in steady state $T_f = u_{in}$ and $T_f = T_{1Q}$.¹⁸ So we have T_{bQ} according to u_{in} , which is the expression that we will use in the LabView program to implement the PI controller :

$$T_{bQ} = \frac{u_{in} - 1,38}{0,94}$$

In practice, the fermentor temperature has to be 53°C for bio-chemical reasons, so u_{in} is set to 53 and $T_{bQ} = 54,91^\circ\text{C}$.

6.4. Performance requirements

As explained in 2.1, the efficiency of the bio-chemical reaction inside the fermentor falls below 51°C and above 55°C . Thus, in case of disturbance, the control system should be able to reach this range of temperature as fast as possible.

Inside this range, the production of biogas reaches its maximum level at the temperature of 53°C . Once the range $51\text{-}55^\circ\text{C}$ reached, the system should then stabilize the fermentor temperature around the steady state of 53°C

¹⁸ Cfr [Example of a non-linear model](#) for more information

Finally, the energy consumption of the system should be considered in the designing. The energy efficiency covers the energy used during steady state as well as the energy used to deal with disturbances. With this in mind, overshoots should be avoided, for energy saving purposes.

The design of the PI will consist of trying to find the PI parameters which best satisfy these requirements. For that purpose, we will examine how the system reacts to some step disturbances from the steady state, for different values of PI parameters. Firstly, we will choose step disturbances of 5°C on the system output T_f . The analysis will be made with the Simulink model and then verified with the real system. According to the model, it has been observed that a PI designed to react to such disturbances is able to deal with smaller disturbances but that the correct reaction to larger disturbances is not guaranteed.

All the analysis will take place with a constant input signal $u_{in} = 53$, since this is the required fermentor temperature in practice. The 200 first seconds of each simulation in Simulink will be used to reach the steady state, and then the disturbance is applied.

6.5. P analysis and the model error

For a start, let's tune the PI controller by using only the proportional component...

$$u_{sp}(t) = K_p \cdot e(t)$$

After several tests with the Simulink model, a value of 3 for the parameter K_p seems to provide quite good results :

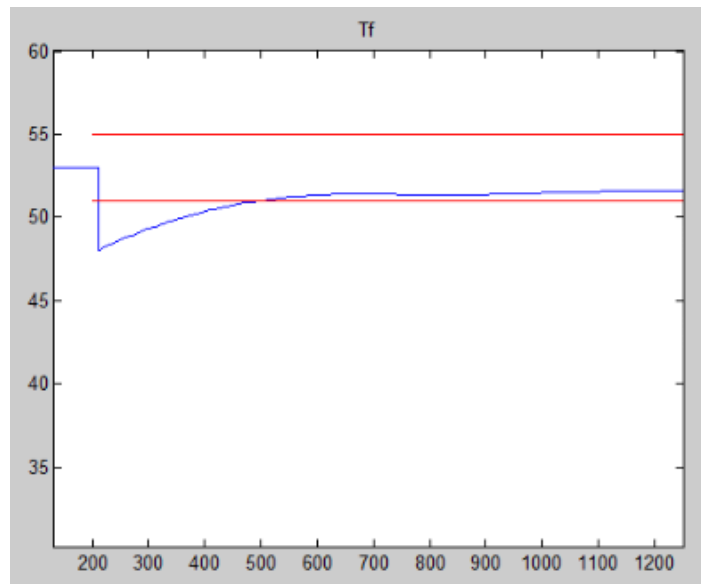


Figure 50 : Model response with $K_p=3$

The range of 51-55°C is reached quite quickly, after around 500s. Of course, the system doesn't reach $T_f = 53^\circ\text{C}$ but we have to remember that the proportional component of a PI controller provides a response which presents a nonzero steady-state error. This drawback should be removed by adding the integrative component.

We can compare this value of K_p to other values in order to understand why this solution is quite good.

For example, with a K_p value of 1, the system is too slow and takes long to reach the 51-55°C range:

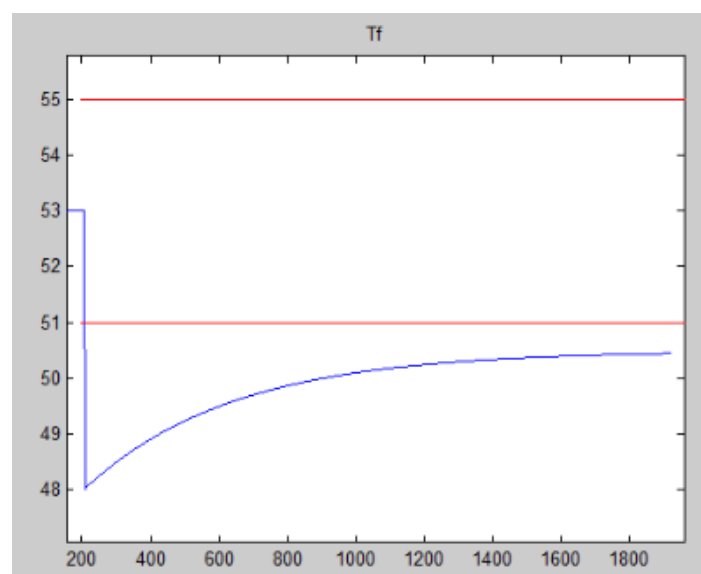


Figure 51 : Model response with $K_p=1$

With a K_p value of 5, the system is quicker but instability increases. We can observe overshoots and we can guess oscillations before the temperature stabilizes:

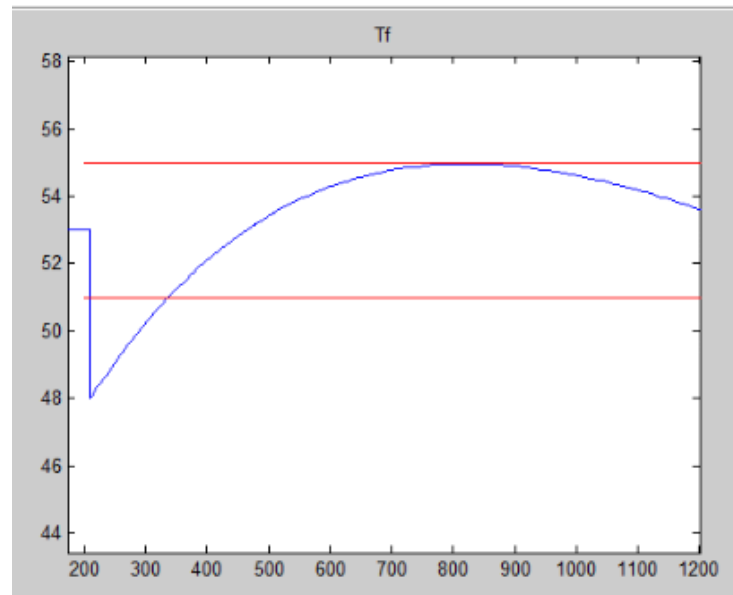


Figure 52 : Model response for $K_p=5$

The next step in our design approach will be to add an integrative component to our PI controller. However, this simulation allows us to discover the first limits of the model, which will show themselves self to be crippling for the designing. Indeed, if we observe the intermediate signals u_{sp} and T_b ,...

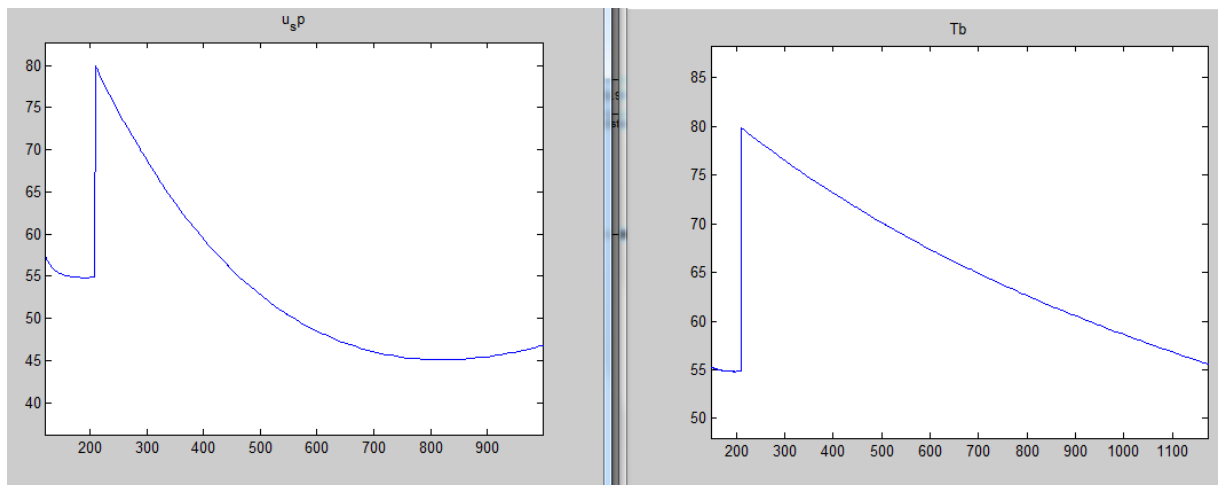


Figure 53 : u_{sp} and T_b model evolution for $K_p=5$

we note two major differences with the real system. First of all, we notice that, in the model, when the boiler is asked to heat up (in this case to 80°C), the boiler temperature T_b is consequently directly increased. In the real plant, this heating up

operation is much slower and it should take considerably more time to increase T_b from 54,91°C to 80°C.

Secondly, the cooling down of the boiler temperature shows itself to be faster than in reality. This model error seems to be due to the calculated value of T_i which appears to be less than in the real operation.

For a fine tuning of the PI controller in the real plant, these two differences with reality should be reduced with an improved. However, given the deadlines set for this project, it has been chosen to continue the PI designing and implementation with the current model in order to provide a first physical control solution in the frame work of this project. Much work has been done to set the current model up and it has been chosen to continue the PI designing in order to prove the student's skills in this area but also to provide a first control solution, which won't be perfect but which should present satisfactory results, particularly in comparison with the previous "valve-controlled" system.

Of course, the current model is not without value. It constitutes an important first step in the frame work of a modeling approach and a base of reflection for a more accurate model. It should be refined by considering that the power P generated at the boiler isn't directly transformed into temperature increase in the boiler. That may be done by tuning the pole of the heater transfer function G_v , in order to find a value which better fits more the reality . Besides, the equation expressing the value of the temperature T_i should be re-examined.

6.6. PI analysis

We are now adding the integrative component to our PI controller.

$$u_{SP}(t) = K_P \cdot e(t) + K_I \cdot \int_0^t e(t) dt$$

The values $K_P = 3$ and $K_I = 0,005$ provide good results:

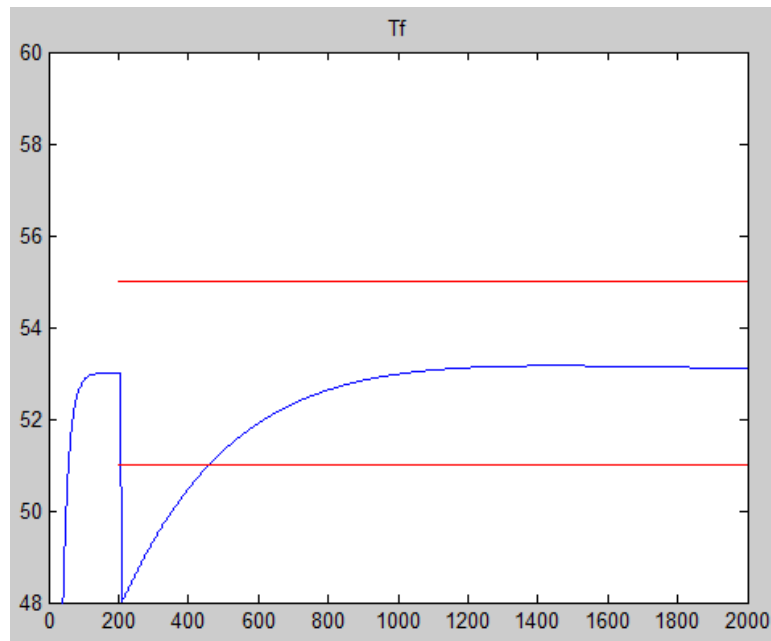


Figure 54: Model response for $K_p=3$ and $K_i=0,005$

The model response reaches the range 51-55°C at a reasonable speed, the overshoot is almost nonexistent and, because of the integrative component, the steady state error should be cancelled out, at least for an infinite time.

We can show that other values of K_i do not provide such good results for $K_p = 3...$

For $K_i = 0,001$, the system becomes considerably slower :

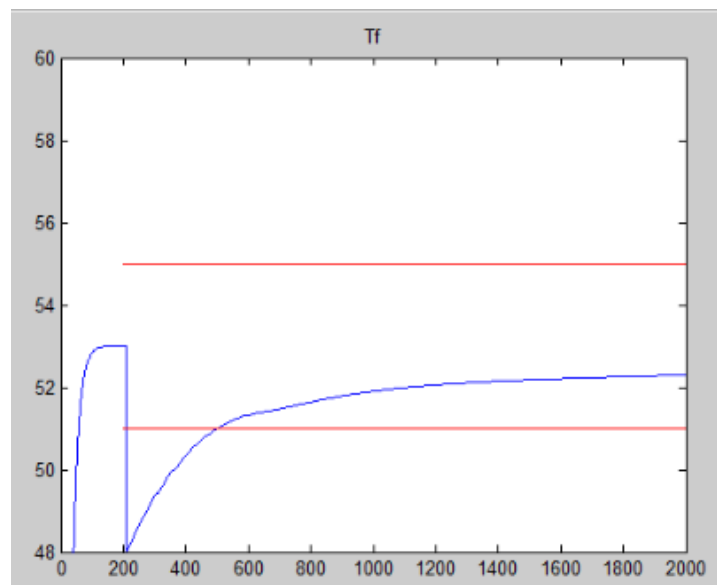


Figure 55: Model response for $K_p=3$ and $K_i=0,001$

And for $K_i = 0,01$, we observe a clear overshoot, which is not good from an energy point of view :

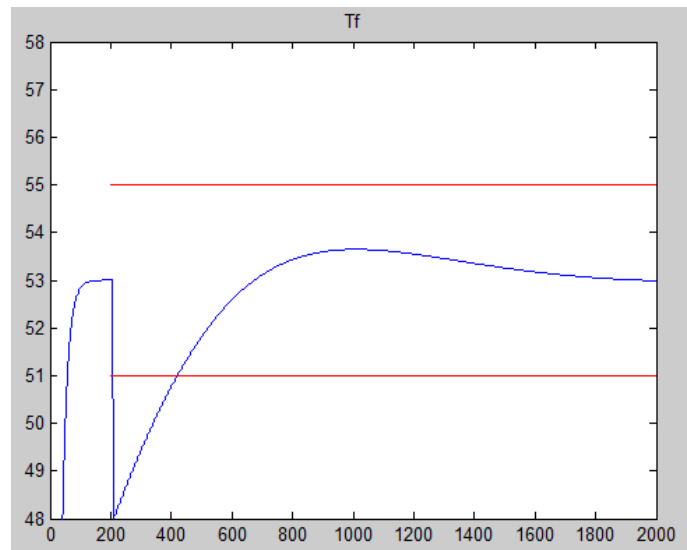


Figure 56: Model response for $K_p=3$ and $K_i=0,01$

That's why the PI controller with the parameters $K_p = 3$ and $K_i = 0,005$ was the first controller to be implemented to the system.

7. Implementation

7.1. Preview

The PI controller has been implemented to the LabView regulation program. LabView acquires the temperature data due to the DAQ card with a sampling time of 1s. The temperature of the fermentor is then used by the PI controller to define the boiler setpoint input. The LabView program is also able to acquire the power consumption of the boiler, which is interesting to have an idea of the energy efficiency of the system. The program is available in Annex 1.

Applying the values $K_p = 3$ and $K_I = 0,005$ to the real system confirmed that the model is quite remote from reality. Indeed, we observe more consequent overshoots, which are drawbacks from both the stability and energy points of view.

These more consequential overshoots can be understood by the fact that the model considers a cooling down of the boiler which is faster than reality. It's easy to heat up the water in the boiler, due to the heating resistance, but the cooling down operation is much harder because all what the system can do is to stop the heating and to wait for the water loop to cool down, with the the ambient air. Now, this cooling down operation is faster in the Simulink model, it is then harder to slow down the temperature evolution in the real system. Moreover, the thermal inertia of the heating resistance is not well modelled (the power generated is directly transformed into temperature): in the real system, the water in the boiler can continue to heat up for a while, even if the power is switched to zero because of the thermal inertia of the heating resistance and this behavior is not simulated by the Simulink model. Besides the overshoots, we can also note that the real plant is slower than the model for the same reasons.

Two steps have been taken in order to limit these overshoots. First of all, the maximum output u_{SP} of the PI controller should be 57. Indeed, in this case and according to the steady state formula (1.1)

$$T_1 = 0,94T_b + 1,38$$

we are sure that the temperature of the fermentor won't exceed 55°C, the upper range limit.

Secondly, when the temperature of the fermentor exceed 53°C, we will force the heating resistance to shut down ($u_{SP}=0$) because that is the best way for the system to cool down. The integrated error value of the integrative component is also reset during this period.

The PI controller modified in this way was able to provide the first satisfactory results.

7.2. First results

Here is the response of the real plant to the same disturbance of -5°C when we apply the PI controller with the parameters $K_p = 3$ and $K_i = 0,005$ and the means previously mentioned to limit the overshoots :

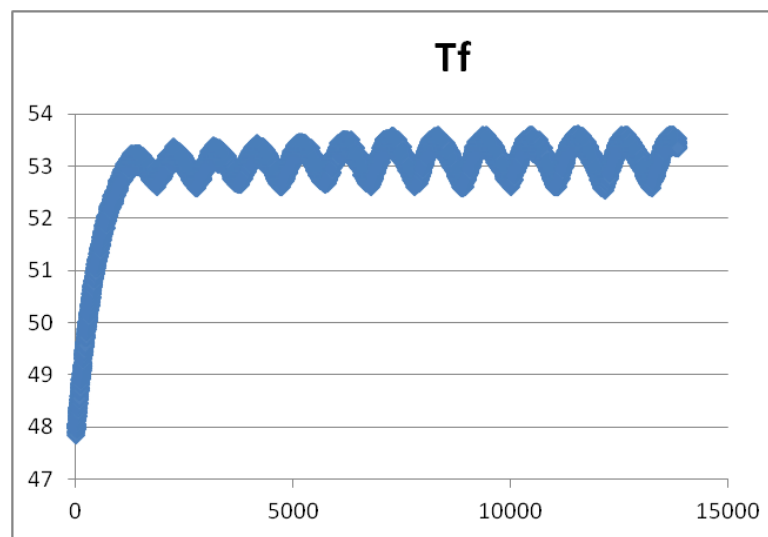


Figure 57: Plant response for $K_p=3$ and $K_i=0,005$

The advantages of this new solution are even more apparent when they are compared to the response of the former control system which was controlled by the valve:

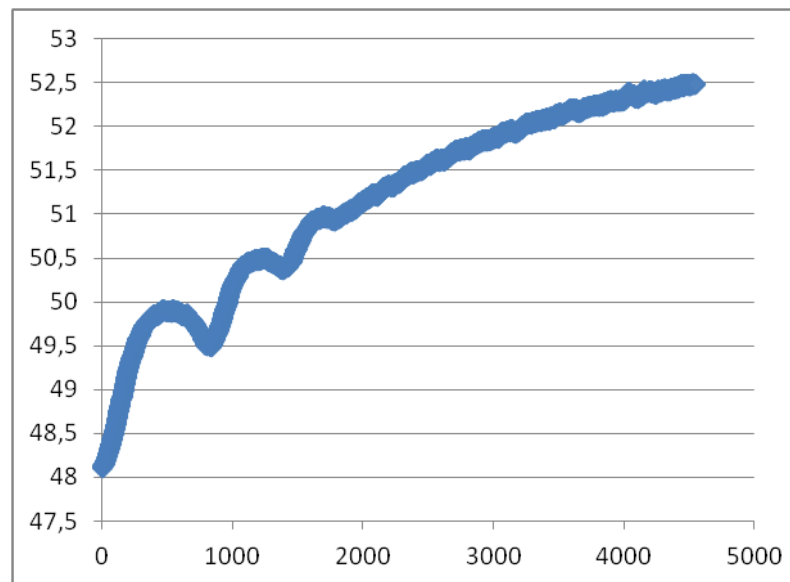


Figure 58: Plant response with the former control system

While the former control system ("valve-controlled") reaches the 51-55°C range in around 1842s (for this sort of test), the new system reaches this range in around 436s only.

The speed of the system is improved and thanks to that, the power consumption is used to react to a disturbance as well. Indeed, between 48 and 51°C the mean power consumption is almost the same: 19,44% of the heater capacity for the new system and 14,99% for the former system. However, the range 51-55°C is reached much faster with the new system and also, this power is used for a much shorter time before reaching the range. So, for this kind of disturbance, the energy used to reach 51°C is about 3,25 times less than it was with the former system.

Concerning the energy consumption during steady state (when the temperature is varies around 53°C), both systems are really similar. According to the tests executed, the new one would consume even a little less: 13,52% of the heater capacity for the new system against 14,77% for the former one. But this difference might be due to the test conditions.

Besides the advantages the new system provides, a drawback appears. Indeed, the following figure shows that the former system was able to stabilize the temperature very close to 53°C ...

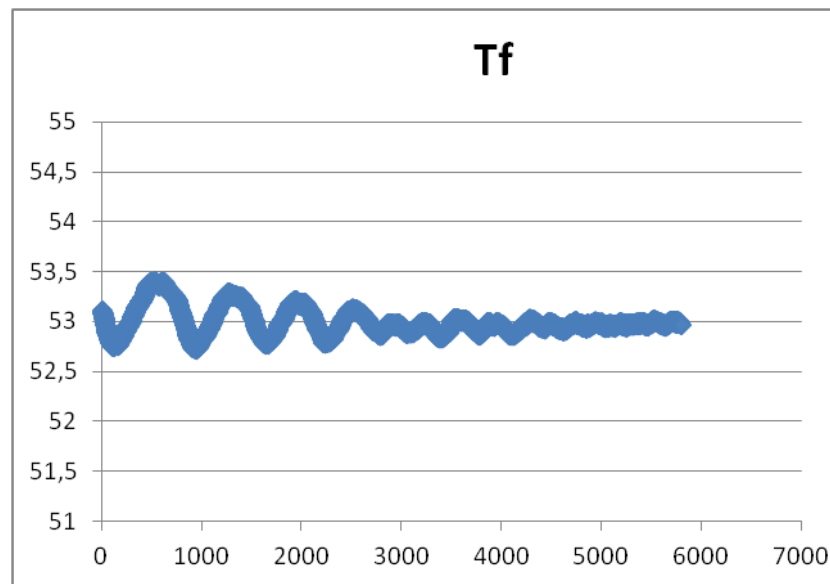


Figure 59 : Plant steady state with the former control system

whereas the new system presents a permanent oscillation :

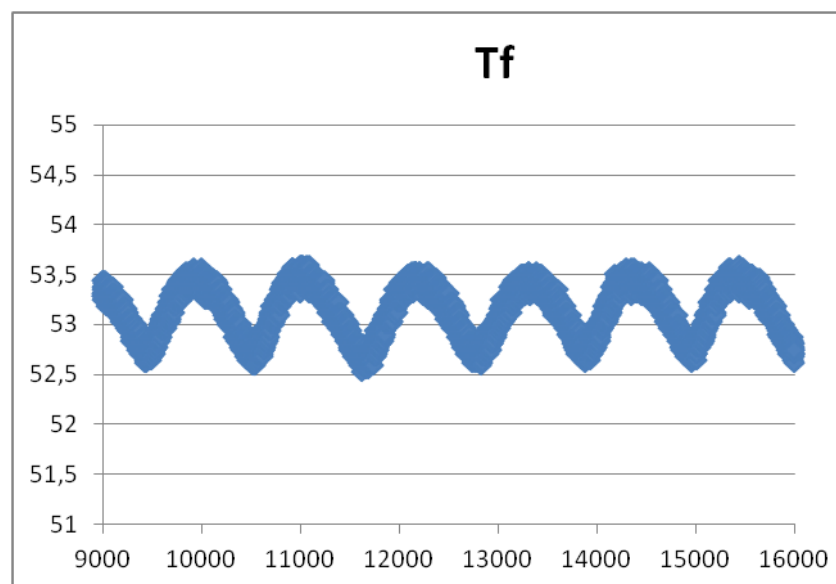


Figure 60 : Plant steady state for $K_p=3$ and $K_i=0,005$

7.3. Trying to improve the design

As shown in the previous figure, the suggested solution presents residual oscillations around 53°C. Even if these oscillations are fairly small and allow the fermentor temperature to stay largely in the 51-55°C range, we could try to improve the solution by reducing these oscillations.

We can see that the residual oscillations present an amplitude varying from 52,5°C to 53,5°C. In order to reduce them, it might be discerning to consider a disturbance of 0.5°C instead of 5°C as previously.

We will try to find the correct PI parameters able to reach precisely 53°C from a disturbance of -0,5°C (i.e. 52,5°C), without any overshoot. This is the purpose of this section.

In order to be sure that the fermentor temperature stabilize when it reaches 53°C, we should take care that the boiler temperature is accurate for this purpose at this moment. In other words, we should make sure that the boiler temperature stabilizes around 54,91°C when the fermentor temperature reaches 53°C, since a 54,91°C boiler temperature provides a 53°C fermentor temperature in the steady state. Because of the time required to run real tests, it was chosen to look for these new PI parameters using the simulations provided by the Simulink model.

After some research, it was found that the parameters $K_p = 2,5$ and $K_i = 0,001$ provide quite good results :

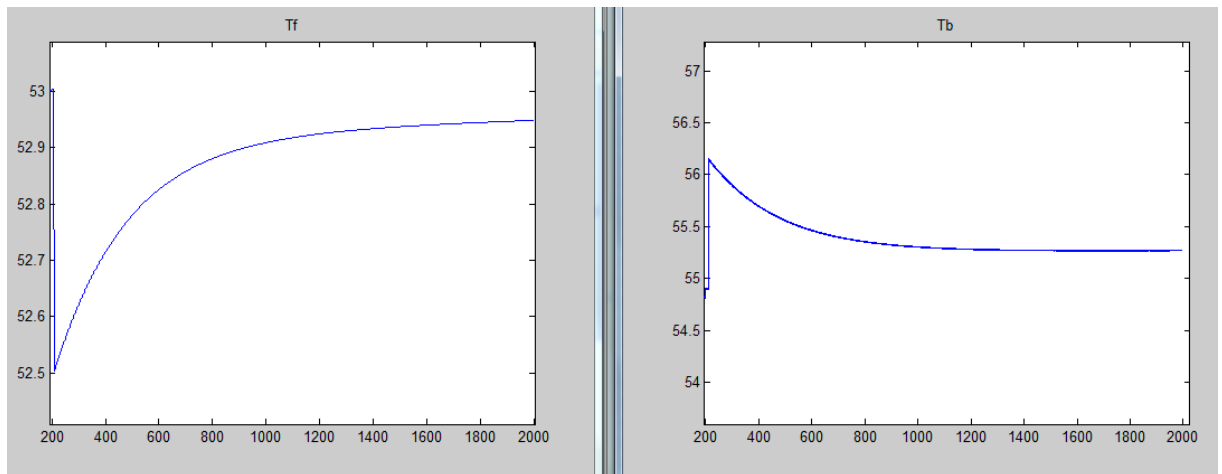


Figure 61: Response of the model for $K_p = 2,5$ and $K_i = 0,001$

1800 seconds after the disturbance, the fermentor temperature is 52,9482°C, approaching 53°C. As for the boiler temperature, it is 55,2720°C, approaching 54,91°C. These first 1800 seconds do not provide an overshoot of the fermentor temperature, which is better than in the previous case. However, if the boiler temperature doesn't have the time to decrease to 54,91°C before the fermentor temperature reach 53°C, we should see a very small overshoot and oscillations till

the boiler temperature stabilizes at 54,91°C. It wasn't possible to complete a test longer than 1800 seconds after the disturbance because of a lack of CPU resources.

We can again show that other PID parameters move the system away from this quite good performance...

Increasing K_I will involve larger overshoots :

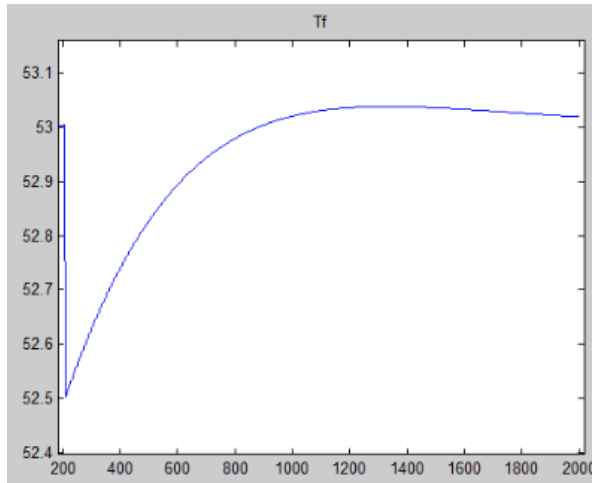


Figure 62: Response of the model for $K_p = 2,5$ and $K_i = 0,005$

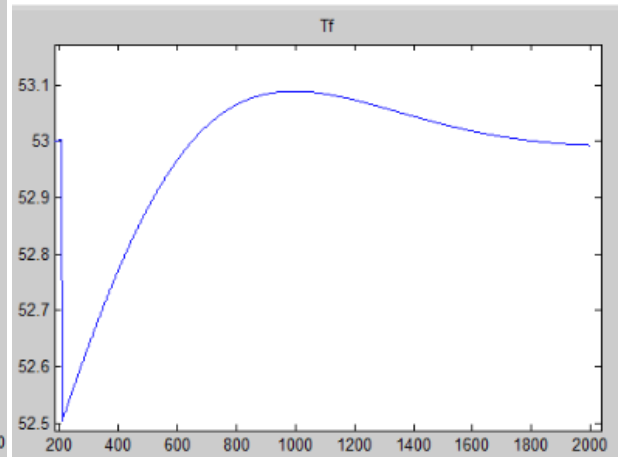
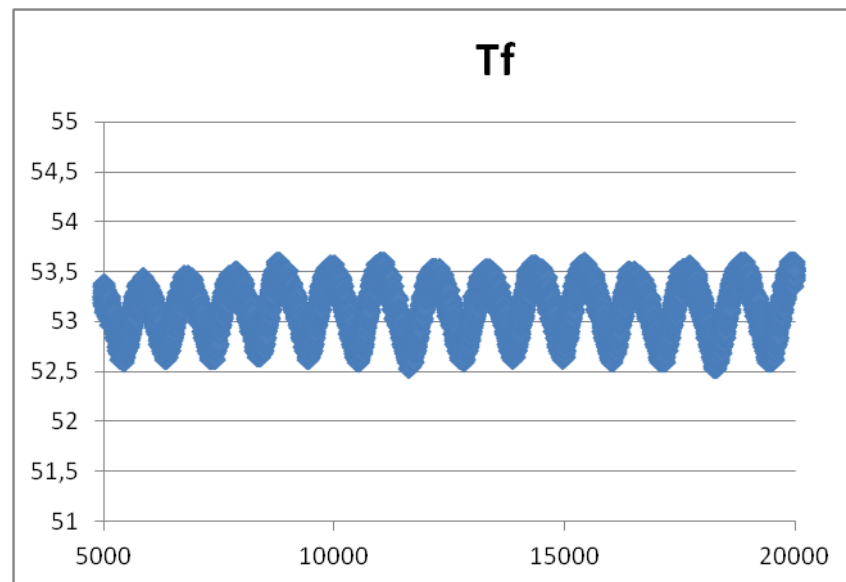


Figure 63: Response of the model for $K_p = 2,5$ and $K_i = 0,01$

Concerning the impact of K_P , trying $K_P = 5$ allows us to observe that the cooling down of the boiler operates less well since $T_b = 55,2731^\circ\text{C}$ after 1800 seconds. Trying $K_P = 1$ shows that the response of the system is less fast, since $T_f = 52,9458^\circ\text{C}$ after 1800 seconds. In both of these cases, the nature of the response is the same.

7.4. Testing the improvements

The PI controller with the parameters $K_P = 2,5$ and $K_I = 0,001$ has been tested on the real plant. The results are shown in the following figure:



No change can be observed compared to the previous solution. The problem we are facing is that the plant behaves differently from the model for the reasons explained in 6.5. It is so difficult to design a PI controller using the model. On the other hand, it is also difficult to design the PI controller using directly the real plant response because a test on the real system takes several hours.

To carry on with fine-tuning the designing of the PI controller, we should improve the model in order to better fit the real plant. However, the current solution has its advantages as presented in 7.2 and proves to be more adapted than the former control system using electro-valve regulation.

Another way to proceed would be to improve the facilities equipment in order to be able to test the system more easily and more quickly.

7.5. Cooling behavior

We can also compare the behavior of the former and new control system when temperature in the fermentor has to be cooled down...

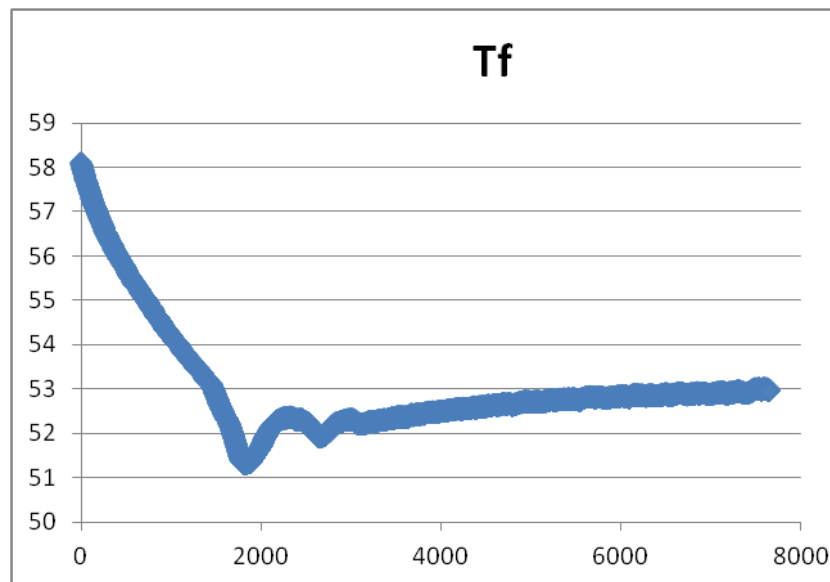


Figure 64 : Cooling behavior of the former system

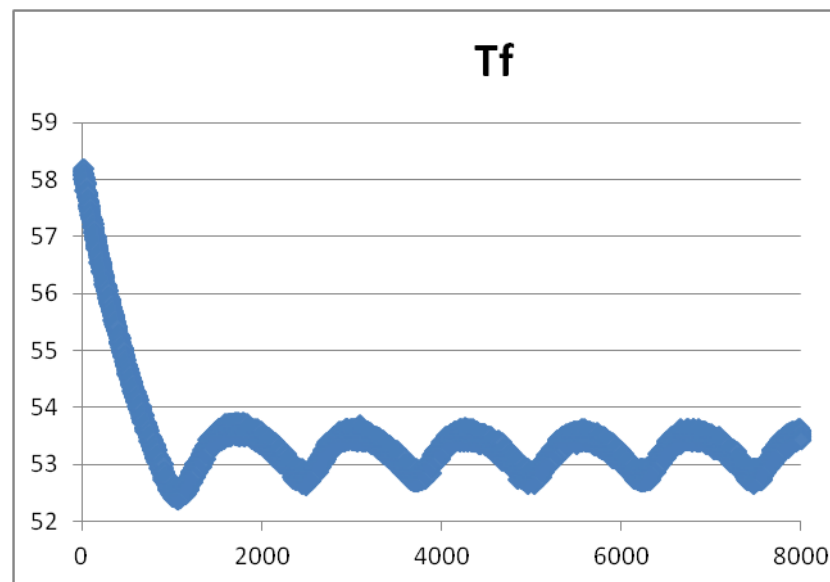


Figure 65: Cooling behavior of the new system

We can see that the cooling operation is faster with the new system. Indeed, the range 51-55°C is reached in 434s, while it was reached in 728s before.

The energy consumption is also reduced during the period: no power is used during the cooling down while 2,86% of the heater capacity was used with the previous control system.

Finally, we observe a smaller undershoot with the new solution : 52,37°C against 51,30°C before.

8. Conclusions

8.1. Results discussion

The project allowed the evaluation of a new strategy of regulation for this biogas demonstration plant. Indeed, while the former system regulated the fermentor temperature by controlling a valve which defines the flow rate of water in the water loop, the new system acts directly on the setpoint of the boiler temperature.

To design and implement this new control system, a model describing the system performance has been established. This model represents the thermal exchange laws occurring in the whole of the system. Even if this model isn't perfect, it is a strong base for analysis purposes in order to design and implement a control solution. This model has been entirely computed in Simulink for analysis purposes.

Two main defects of the model were successfully detected. First of all, the thermal exchange occurring at the heater level is not well simulated. Indeed, according to the model, when power is applied to the heating resistance, it is directly converted into heat in boiler. In the reality, the thermal transfer isn't immediate and the energy needs time to pass from the resistance to the water. To improve the model on this point, the pole of the heater transfer function should be tuned in order to find a value which better fits the facts.

The second defect is that simulation of the temperature at the input of the boiler is noticeably colder than in reality. The result is that the cooling of the boiler is appreciably faster for the model than in reality. Particular attention should be paid to this temperature modeling in order to improve the accuracy of the model.

These two defects showed themselves to be crippling for the design and the implementation of the controller. But nevertheless, a control solution has been implemented, using the boiler control and the LabView software. This solution presents significant advantages compared to the former control system. Indeed, the speed of response to disturbances is largely increased. The result of this is also decreased energy consumption when the system faces disturbances because power

is used to deal with these disturbances for a shorter time. In steady state, both the former and the new control systems consume almost the same amount of energy.

During steady state, the new solution presents oscillations of $\pm 0.5^{\circ}\text{C}$ around 53°C . A new design has been experimented on to remove this drawback but it is not easy with the current model. To tune the PI controller more finely, the model should be improved, particularly concerning the two defects previously mentioned.

The new solution arising from this project has also the advantage of not adding pressure losses to the water loop (the electro-valve isn't used anymore), so the pump doesn't have to compensate for these pressure losses and energy saving is generated.

It should be kept in mind that the demonstration system uses water inside the fermentor and that the approach should be adapted for the actual production of biogas.

Finally, a control solution using both boiler control and valve control could be considered. It might provide results combining the advantages of each case.

To conclude, we can say that a first strong model has been established to simulate the system in operation. This model represents a first step in the framework of more accurate modeling. A control solution has been implemented on the real plant and the results have shown obvious advantages compared to the former system. The drawback of this new solution has been detected and it has been established that it should be corrected thanks to a new design based on a more accurate model. The two main defects of the model were detected in order to show the way forward to model improvements.

8.2. Personal assessment

This first regulation project has been a good opportunity for the student to refresh and improve his knowledge in the field of regulation, notably with the different reference books used during this project.

This thesis required the student to prove his skills in various fields such as Thermal Exchange, Chemistry, Pump Theory, Electronics, Numerical Analysis, Mathematics, MatLab software and, of course, Regulation. This point is particularly important for studies which claim to be polyvalent.

Discovering and learning the basics of the LabView and Simulink software are also an asset for the future and a good experience in autodidacticism, within a concrete background.

This project required also the student to show his aptitudes in terms of autonomy, conceptualization, initiatives, innovating skills, critical thinking, ... This project tries to present an engineer's approach to a technical issue and to reveal the student's skills in this field.

Finally, the context of this internship at Aalborg University, Esbjerg campus in Denmark, allowed the student to significantly improve his level of English. This is also an important asset, considering the importance of the knowledge of English worldwide and especially in the world of work.

Annex

Annex 1 : Programs Files

Cf. Flash Drive or CD.

- Biogas_boiler_pid.vi : The new LabView control solution
- Biogass_power.vi : The former LabView control solution, with boiler power acquisition.
- JULABO-Device-Driver.zip : The JULABO library for LabView
- Closed_loop_toworkspace.mdl : The Simulink Model (run simplification.m before in order to initialize the variables)
- G_identification.m : MatLab algorithm to find U
- Air_test.m : MatLab algorithm to find G_c

Annex 2 : Example of a Non-linear Model

Here is the paragraph where the work on non-linear models is highlighted.

Linearization:

$$c_w \cdot M_b \cdot s \cdot T_b = -c_w \cdot \dot{m} \cdot (T_b) + \frac{\mathcal{L}[V^2]}{R} - U_b(T_b) \cdot A_b$$

We are going to linearize the previous expression around a given operating point (V_q, T_{b_q}) .

Let's come back to the time domain, using the inverse Laplace transform:

$$\frac{c_w \cdot M_b \cdot dT_b}{dt} = c_w \cdot \dot{m} \cdot (-T_b) + \frac{V^2}{R} - U_b(T_b) \cdot A_b$$

Letting $x = y = T_b$ and $u = V$, we find a couple of equations

$$\frac{dx}{dt} = -\frac{(c_w \cdot \dot{m} + U_b \cdot A_b)}{c_w \cdot M_b} \cdot x(t) + \frac{u^2(t)}{R \cdot c_w \cdot M_b}$$

$$y(t) = x(t)$$

that can be easily linearized around the point Q characterized by $(u_q, x_q) = (V_q, T_{bq})$, according to the reference book¹⁹ :

$$\frac{d\Delta x(t)}{dt} = A. \Delta x(t) + B. \Delta u(t)$$

$$\Delta y(t) = C. \Delta x(t) + D. \Delta u(t)$$

With

$$A = \left. \frac{\partial \left(-\frac{(c_w \cdot \dot{m} + U_b \cdot A_b)}{c_w \cdot M_b} \cdot x(t) + \frac{u^2(t)}{R \cdot c_w \cdot M_b} \right)}{\partial x} \right|_{\substack{x=x_q \\ u=u_q}} = -\frac{(c_w \cdot \dot{m} + U_b \cdot A_b)}{c_w \cdot M_b}$$

$$B = \left. \frac{\partial \left(-\frac{(c_w \cdot \dot{m} + U_b \cdot A_b)}{c_w \cdot M_b} \cdot x(t) + \frac{u^2(t)}{R \cdot c_w \cdot M_b} \right)}{\partial u} \right|_{\substack{x=x_q \\ u=u_q}} = \frac{2}{R} \cdot \frac{u_q}{c_w \cdot M_b}$$

$$C = \left. \frac{\partial(x(t))}{\partial x} \right|_{\substack{x=x_q \\ u=u_q}} = 1$$

$$D = \left. \frac{\partial(x(t))}{\partial u} \right|_{\substack{x=x_q \\ u=u_q}} = 0$$

Finally, the transfer function of this small-signal model is given by the formula (1.23):

$$G_V(s) = \frac{\mathcal{L}[\Delta x(t)]}{\mathcal{L}[\Delta u(t)]} = \frac{\mathcal{L}[\Delta T_b(t)]}{\mathcal{L}[\Delta V(t)]} = C(sI - A)^{-1}B + D = \frac{\frac{2}{R} \cdot \frac{V_q}{c_w \cdot M_b}}{s + \frac{(c_w \cdot \dot{m} + U_b \cdot A_b)}{c_w \cdot M_b}} = \frac{K_V}{s - p_V}$$

With

$$K_V = \frac{2}{R} \cdot \frac{V_q}{c_w \cdot M_b} ; p_V = -\frac{(c_w \cdot \dot{m} + U_b \cdot A_b)}{c_w \cdot M_b} = p'$$

¹⁹ (GOODWIN, et al., 2001)

As mentioned, in the reference book : "*The linearization procedure presented above produces a model that is linear in the **incremental** components of inputs and outputs around a chosen operating point (i.e., small-signal model)*".²⁰

So, linearization leads to a small-signal model where the incremental components of the signals around Q have to be used, instead of the signals themselves. That's why we have to use the following general scheme:

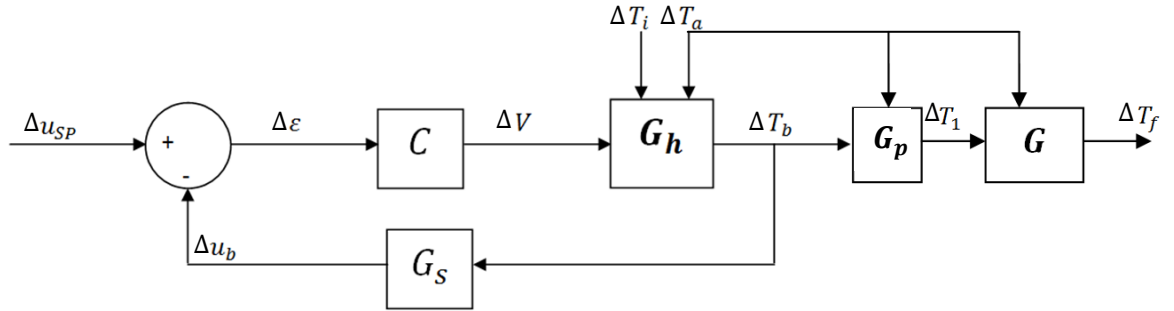


Figure 66: Small-signal control scheme of the global system

Where the operator Δ applied on the signal v means the difference between the original signal and the operating value : $\Delta v = v - v_Q$.

To use this scheme, and to determine G_v , we need to choose a proper operating point Q and to determine the value of each signal in Q.

Q identification :

To be of use, the point Q has to symbolize the normal constant operating point. That's why Q will be chosen so as to produce a constant temperature in the fermentor equal to $T_{fQ} = 53^\circ\text{C}$, with a ambient temperature $T_{aQ} = 23^\circ\text{C}$. So, the value in Q of each signal will be the constant value of this signal which produces T_{fQ} in the system.

T_{1Q} can be deduced from the equation (1.24)

²⁰ (GOODWIN, et al., 2001)

$$T_f(t) = T_{f_0} \cdot e^{pt} + (K_1 \cdot T_1 + K_a \cdot T_a) \frac{e^{pt} - 1}{p}$$

by considering the point Q ($t = \infty$, because is a constant operating point) :

$$T_{1Q} = \frac{-p \cdot T_{fQ} - K_a \cdot T_{aQ}}{K_1} = 53^\circ\text{C}$$

For T_{bQ} , we know from the ATC configuration that the relation between T_1 and T_b is given by the equation (1.1), for a temperature $T_a = 23^\circ\text{C}$:

$$T_{1Q} = 0,94T_{bQ} + 1,38 \Rightarrow T_{bQ} = 54,91^\circ\text{C}$$

V_Q is determined by means of a test : we set u_{SP} for the boiler to keep $T_{bQ} = 54,91^\circ\text{C}$, using the integrated PID controller. Then, we are able to obtain, via LabView, the power used by the heater to deduce V_Q in the normal constant operating state.

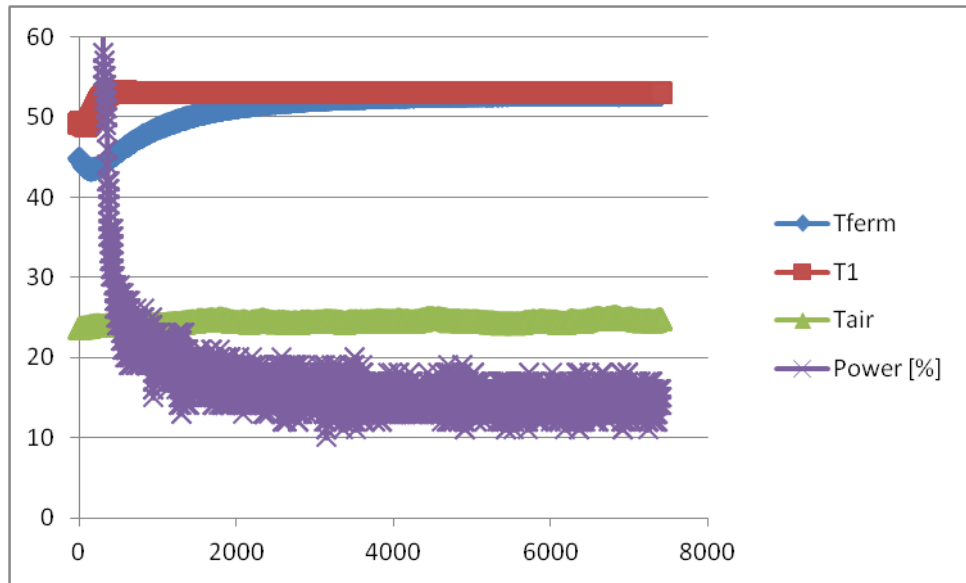


Figure 67: Q determination test

We see that, to guarantee the normal state, the power used by the heater has to be 14,92% of the maximum power (which is 2000W).

$$P_Q = 2000 \cdot 14,92\% = 298,4 \text{ W}$$

$$V_q = \sqrt{P_Q \cdot R} = 88,84 \text{ V}$$

where R is deduced from the maximal boiler power and the voltage used in this

$$\text{case: } R = \frac{V^2}{P} = \frac{230^2}{2000} = 26.45 \, \Omega$$

T_{iQ} can also be deduced from this test. Indeed, from the equation (1.27),

$$\frac{c_w \cdot M_b \cdot dT_b}{dt} = c_w \cdot \dot{m} \cdot (T_i - T_b) + \frac{V^2}{R} - U_b(T_b - T_a) \cdot A_b$$

We have, in Q :

$$T_{iQ} = \frac{-\frac{V^2}{R} + U_b(T_{bQ} - T_{aQ}) \cdot A_b}{c_w \cdot \dot{m}} + T_{bQ} = 51,75 \, ^\circ\text{C}$$

because $\left. \frac{dT_b}{dt} \right|_Q = 0$, since Q is a constant operating point.

Finally, we can now calculate the gain and the pole of G_V :

$$K_V = \frac{2}{R} \cdot \frac{V_q}{c_w \cdot M_b} = 1.529817207593690e - 004$$

$$p_V = p' = -0.001965014618225$$

Annex 3 : List of Tasks Completed

Here is a non-exhaustive list of the tasks executed:

- Reading the book : VETCOUR N., *Automatique : regulation IG4*, Liège, 2011-2012
- Library introduction
- Learning simulink basics with a tutorial
- Reading the introduction (100p) of the book : GOODWIN C., GRAEBE S., SALGADO E., *Control System Design* , Prentice Hall, Upper Saddle River, New Jersey, 2001.
- Learning LabView basis with a tutorial
- Choice of the project
- Security rules for the bioenergy lab presentation
- Reading manual of the system
- Manual tests with the circulation bath and the PI controlled valve
- Fixing first objectives of the thesis
- Searching information about biogas

- Writing the report n°1
- Controlling the electro-valve via LabView
- Understanding of the existing LabView program
- Problem identification : Finding a new strategy for the control of the system
- Meetings with the mentor
- Making the RS-232 cable
- Establishing communication between LabView and the Boiler
- First Fermentor Model Development
- Determining the parameters of the First Fermentor Model
- Programmation for data acquisition from the boiler and the sensors
- Calibration of the boiler
- Reading the second part (100p) of the book : GOODWIN C., GRAEBE S., SALGADO E., *Control System Design* , Prentice Hall, Upper Saddle River, New Jersey, 2001.
- Second Fermentor Model Development
- Finding the fermentor transfer function expression
- Boiler Model Development
- Attempt to determine the fermentor parameters with *optimtool*
- Writing the report n°2
- Determining the fermentor parameters with the System Identification Tool
- Linearization of a non linear Model
- Contacts with Julabo for technical support
- Whole Model Development
- Implementing the model in Simulink and verification
- Simulink understanding
- PI design with Simulink
- Tests on the real plant
- Trying to improve the solution
- Writing thesis

Bibliography

Works

DEMIBRAS, A. 2009. *Biofuels : Securing the Planet's Future Energy*. London : Springer, 2009.

GOODWIN, C., GRAEBE, S. and SALGADO, E. 2001. *Control System Design*. Upper Saddle River, New Jersey : Prentice Hall, 2001.

HAUGEN, F. 1997. *Learn Simulink 2 in 3 hours !* Porsfrunn, Norway : TechTeach, 1997.

HOLM-NIELSEN, J.B., AL SEADI, T. and OLESKOWICZ-POPIELP, P. 2009. The Future of Anaerobic Digestion and Biogas Utilization. *Bioresource Technology*. 2009.

http://fr.wikipedia.org/wiki/Biogaz#Sources_de_biogaz. *www.wikipedia.org*. [Online]

KELNER, V. 2011. *Transfert de Chaleur*. Liège : Helmo Gramme - Unité Energie, 2011.

LOUSBERG, P. 2009. *Mathématiques au Service de l'Ingénieur : Analyse Numérique*. Liège : Helmo Gramme, 2009.

MESSE, J.Y. 2002. Eau, masse volumique, enthalpie, viscosité spécifique, pression atmosphérique, vapeur saturante. *ThermExcel*. [Online] ThemExcel, April 2002.
http://www.thermexcel.com/french/tables/eau_atm.htm.

NationalInstrument. 2007. *Getting Started with LabView*. Austin, Texas : National Instruments, 2007.

ROETZEL, W. and SPANG, B. 2010. C2 Overall Heat Transfer. [book auth.] P. STEPHAN, et al. *VDI Heat Atlas*. Berlin Heidelberg : Springer, 2010.

VETCOUR, N. 2011-2012. *Automatique : Régulation (IG4)*. Liège : Helmo Gramme, 2011-2012.

Wikis:

<http://fr.wikipedia.org/wiki/Biom%C3%A9thane>

http://en.wikipedia.org/wiki/Natural_gas

http://en.wikipedia.org/wiki/Anaerobic_digestion

<http://fr.wikipedia.org/wiki/Fermentation>

http://fr.wikipedia.org/wiki/Carburants_verts#Premi%C3%A8re_et_deuxi%C3%A8me_g%C3%A9n%C3%A9rations